UNIVERSITY OF CALIFORNIA,
IRVINE

Methodology to Assess Emissions and Performance Trade-offs for Retrofitted Alternative Fuel-Powered Short, Medium, and Long Haul Aircraft

THESIS

submitted in partial satisfaction of the requirements
for the degree of

MASTER OF SCIENCE

in Mechanical and Aerospace Engineering

by

Melody Emmanouilidi

Thesis Committee:
Professor Jacqueline Huynh, Chair
Professor Jack Brouwer
Professor Haithem A. Taha

2023

TABLE OF CONTENTS

Page

LIST OF FIGURES **iii**

LIST OF TABLES **iv**

ACKNOWLEDGMENTS **v**

ABSTRACT OF THE THESIS **vi**

NOMENCLATURE **1**

1 Introduction **4**

2 Methodology for Assessing Emissions and Performance Trade-offs **7**
2.1 Flight Profile Module 9
2.1.1 Tank Configuration Module 13
2.1.2 Center of Gravity Model 16
2.1.3 Emissions Module 18
2.1.4 Environmental Impacts Module 21

3 Methodology Demonstration for Alternative Fuel Retrofit on Short, Medium, and Long Haul Aircraft **25**
3.1 Analysis of Results 27
3.1.1 Tank Design and Interior Layout 29
3.1.2 Cost for Short, Medium, and Long Haul Configurations 40
3.1.3 Emissions and Lifecycle Analysis for Short, Medium, and Long Haul Configurations 44
3.1.4 Overall Aircraft Weight Change 51
3.1.5 Comparison Between Commercial and Business Aircraft Results . . . 56

4 Conclusion **58**

Bibliography **61**

LIST OF FIGURES

Page

2.1 Modeling framework of the methodology to assess emissions and performance trade-offs for a retrofitted SOFC hybrid and H_2 Powered Aircraft 8
2.2 Design changes to the engine due to the different properties of hydrogen . . . 10
2.3 Addition of a heat exchanger for the cryogenic liquid fuel combustion 10
2.4 Power train SOFC hybrid for short, medium and long haul aircraft designed for fuel cell hybrid 12
2.5 Tank configuration module flowchart [13] 13
2.6 H_2 Cryogenic Tank geometry definition 16
2.7 Lifecycle Assessment (LCA) boundary of Jet-A Fuel (Top) and LH_2 fuel (Bottom) 23

3.1 Cross section of short haul fuselage: (Left) H_2-combustion (Right) SOFC hybrid combustion 31
3.2 Side view layouts for short haul retrofit analysis 32
3.3 Cross section of medium haul fuselage: (Left) H_2-combustion (Right) SOFC hybrid combustion 35
3.4 Side view layouts for medium haul retrofit analysis 35
3.5 Cross section of long haul fuselage: (Left) H_2-combustion (Right) SOFC hybrid combustion 38
3.6 Side view layouts for long haul retrofit analysis 39
3.7 CO_2, CO, HC, NO_x, and H_2O emissions per segment of conventional kerosene for short haul (Top), medium haul (Middle), and long laul (Bottom) aircraft 45
3.8 CO_2, CO, HC, NO_x, and H_2O emissions per segment of H_2-combustion for short haul (Top), medium haul (Middle), and long haul (Bottom) aircraft . . 46
3.9 CO_2, CO, HC, NO_x, and H_2O emissions per segment of SOFC hybrid powered short haul (Top), medium haul (Middle), and long haul (Bottom) aircraft . . 47
3.10 Resulting fractional weights from implementing a retrofit on a H_2-combustion (Left) and a SOFC hybrid (Right) powered Embraer 170LR 53
3.11 Resulting fractional weights from implementing a retrofit on a H_2-combustion (Left) and a SOFC hybrid (Right) powered Boeing 737-800 54
3.12 Resulting fractional weights from implementing a retrofit on a H_2-combustion (Left) and a SOFC hybrid (Right) powered Boeing 777-300ER 55

LIST OF TABLES

Page

2.1 Power train for SOFC hybrid 11
2.2 Assumed flight profile segments medium, short, and long haul [25][26] 20

3.1 Aircraft performance specifications [18], [19], [20] 26
3.2 Fuel weights for cruise 27
3.3 Power and SOFC energy requirements 28
3.4 Cryogenic LH_2 tanks for short haul H_2-combustion 30
3.5 Cryogenic LH_2 tanks for short haul SOFC hybrid combustion 31
3.6 SOFC power train for short haul SOFC hybrid combustion 31
3.7 Cryogenic LH_2 tanks for medium haul H_2-combustion 33
3.8 Cryogenic LH_2 tanks for medium haul SOFC hybrid combustion 34
3.9 SOFC power train for medium haul SOFC hybrid combustion 34
3.10 Cryogenic LH_2 tanks long haul H_2-combustion 37
3.11 Cryogenic LH_2 tanks for long haul SOFC hybrid combustion 38
3.12 SOFC power train for long haul SOFC hybrid combustion 38
3.13 Required refuel stops for fixed range 40
3.14 Fuel cost of all configurations 41
3.15 Cryogenic tank cost of H_2-combustion and SOFC hybrid configurations . . . 42
3.16 Capital cost of SOFC power train configurations 42
3.17 Total cost of all configurations 43
3.18 NO_x and H_2O total emissions for short, medium, and long haul aircraft . . . 44
3.19 CO_2 emissions for full lifecycle analysis of all configurations 48
3.20 % Difference between WTW short haul lifecycles 49
3.21 % Difference between WTW medium haul lifecycles 50
3.22 % Difference between WTW long haul lifecycles 51
3.23 % Mass difference between retrofitted and conventional powered aircraft . . . 52

ACKNOWLEDGMENTS

I wish to express my heartfelt appreciation to my advisor, Professor Jacqueline Huynh, for her unwavering devotion, support, and guidance during my graduate years at the University of California, Irvine.

I would also like to extend my gratitude to Professors Haithem E. Taha and Jack Brouwer for their contributions as members of my MS committee.

Lastly, I am deeply grateful to my parents for their unconditional and unwavering support throughout my educational pursuits.

Portions of chapter 2 of the text in this thesis are reprints of the material as it appears in the AIAA Scitech 2022 publication "Methodology for Assessing Retrofitted Hydrogen Combustion and Fuel Cell Aircraft Environmental Impacts", co-authored by Khaled AlSamri and Jessica De la Cruz.

This work was sponsored by the Aircraft and Systems Laboratory (ASL) at the University of California Irvine. Opinions, interpretations, conclusions, and recommendations are those of the author and are not necessarily endorsed by the United States Government.

ABSTRACT OF THE THESIS

Methodology to Assess Emissions and Performance Trade-offs for Retrofitted Alternative Fuel-Powered Short, Medium, and Long Haul Aircraft

By

Melody Emmanouilidi

Master of Science in Mechanical and Aerospace Engineering

University of California, Irvine, 2023

Professor Jacqueline Huynh, Chair

Hydrogen (H_2) combustion and Solid Oxide Fuel Cells (SOFC) have the potential to mitigate aviation-induced greenhouse emissions in comparison to kerosene propulsion. This thesis describes a methodology to assess the performance and emissions trade-offs of retrofitting a short, medium, and long haul aircraft employing conventional kerosene powered propulsion, with H_2-combustion and SOFC hybrid powered lower emission alternatives. The proposed framework employs a constant range approach analysis to design a liquid hydrogen fuel tank that meets insulation, sizing, center of gravity, and power constraints. These liquid hydrogen tanks are utilized to compare the performance of H_2-combustion powered and SOFC hybrid powered aircraft, all flying the same range. A lifecycle assessment is conducted to evaluate the potential mitigation of carbon footprints through greenhouse gas emissions and contrail formation effects. Additionally, a cost analysis is modeled to examine the implications of implementing such retrofitting. In this thesis, three sample cases are presented to demonstrate the proposed framework on different aircraft models: Embraer 170LR (representing short haul), Boeing 737-800 (medium haul), and Boeing 777-300ER (long haul). The advantages of adopting the mentioned alternative fuel sources are evident, with an overall reduction in aircraft mass observed for medium and long haul configurations. However, for the short haul case, there is a slight increase in overall weight of 1.13% for H_2-combustion

and 1.39% for the SOFC hybrid system. Conversely, the medium haul case shows a substantial 27.73% decrease in overall weight for H_2-combustion and a 0.4% decrease for the SOFC hybrid configuration. For long haul flights, H_2-combustion and SOFC cases yield weight reductions of 38.51% and 2.85%, respectively, compared to conventional kerosene-powered aircraft. Moreover, considering the trade-off of removing cargo compartments to maintain fixed passenger capacity and range by making refueling stops, the lifecycle analysis of green hydrogen in H_2-combustion and SOFC hybrid configurations results in an average reduction of 40% and 68% in CO_2 lbs of emissions, respectively, compared to conventional Jet-A fuel emissions across all haul configurations. Fuel costs increase by 45% when replacing kerosene combustion with SOFC hybrid power using gray H_2 for the short haul configuration, considering one refueling stop. In the case of long haul flights using green H_2-combustion, the cost increases by 58.18% compared to conventional kerosene powered aircraft. However, for the long haul SOFC green H_2-combustion case (ii), which includes 50% of passengers and their luggage, the total cost is estimated to be close to 33 million USD, representing a 98.90% increase compared to the cost of the long haul kerosene-powered aircraft. The results obtained through this methodology indicate that retrofitting all three aircraft to operate with these alternative fuels can significantly lower carbon emissions at a higher total cost, considering the trade-off of removing cargo compartments and making refueling stops to maintain the same fixed range as specified for each aircraft.

NOMENCLATURE

$C_{p,Air}$	=	Specific Heat Capacity of Air
d	=	Height of the Spherical Head
d_1	=	Width of Spherical Head
d_o	=	Radius of Inner Tank
$EI(X)$	=	Emission Index of Species X
e_w	=	Weld Efficiency
FOS	=	Factor of Safety
g	=	Acceleration due to Gravity on Earth
G	=	Mixing Line Slope
h	=	Cruising Altitude
H	=	Hydrogen
h_f	=	Heat Energy Available per Unit Weight of Fuel
K	=	Geometrical Constant
K_{ins}	=	Thermal Conductivity of Insulation
L	=	Length of the Cylindrical Part of Tank
λ_{tank}	=	Total Length of Tank
L_{cyl}	=	Length of Cylinder
LHV_{fuel}	=	Lower Heat Value of Fuel
LH_2	=	Liquid Hydrogen Fuel
L/D	=	Lift-to-Drag Ratio

$M_{boiloff}$	=	Mass Boiloff
$m_{filledcapsule}$	=	Mass of Filled Capsule
M_H	=	Mass of Hydrogen
m_t	=	Mass of Tank
$\dot{m}_{air}$	=	Mass Flow Rate of Air
$\dot{m}$	=	Mass Flow Rate
$\dot{m}_{fuel}$	=	Mass Flow Rate of Fuel
$\dot{m}_{H_2}$	=	Mass Flow Rate of Hydrogen
$\dot{m}_{H_2O}$	=	Mass Flow Rate of Water
$\dot{m}_{steam}$	=	Mass Flow Rate of Steam
MAC	=	Mean Aerodynamic Chord
NU_D	=	Nusselt Number
P	=	Pressure
P_a	=	Ambient Pressure at Altitude
P_{des}	=	Pressure for Hydrogen Storage
Pr	=	Prandtl Number
q	=	Heat Loss
Q	=	Heat Transfer Rate
r	=	Radius
r_1	=	Radius of Inner Vessel
r_2	=	Radius of Outer Shell
r_{ins}	=	Radius of Insulation
R	=	Range
Re_d	=	Reynolds Number
T	=	Temperature
T_o	=	Outside Temperature
T_i	=	Inside Temperature

T_1	=	Outside Temperature
T_2	=	Inside Temperature
t_w	=	Wall Thickness
t_{wh}	=	Wall Hemisphere Thickness
TWW	=	Tank-to-Wheel
V_i	=	Excess Volume
V_t	=	Tank Volume
V_{out}	=	Volume Out
V_{system}	=	Volume of tank system
WTT	=	Well-to-Tank
WTW	=	Well-to-Wheel
W_{to}	=	Maximum Takeoff Weight
W_{fuel}	=	Fuel Weight
ϵ_{H_2O}	=	Molar Mass of Water over Mass of Dry Air
$\eta_{overall}$	=	Overall Engine Efficiency
λ_t	=	Tank Sizing Constraints
λ_{cabin}	=	Tank Sizing Cabin Constraints
σ_a	=	Tensile Strength of Material for Cryogenic Tank
ρ	=	Density
τ_{allow}	=	Allowable Shear Stress
$()_h$	=	Property at Altitude
$()_{st}$	=	Property at Standard Temperature
$()_{H_2}$	=	Property for Hydrogen
$()^*$	=	Per Segment

Chapter 1

Introduction

In the field of aviation, aircraft are categorized into several classifications based on their ability to cover distances without requiring refueling. This categorization covers short, medium, and long haul aircraft, each designed to fulfill various travel needs. Short haul aircraft are built for flights between 950 to 2500 nautical miles [1]. These aircraft are mainly used for regional or domestic flight demands. Medium haul aircraft, on the contrary, offer an increased flight range, which allows traveling distances from 2500 to 4,500 nautical miles [1]. These aircraft are frequently used for intercontinental or inter-regional journeys, including the gaps between continents or regions. Lastly, long haul aircraft possess the longest flight endurance, capable of traveling distances of from 4500 nautical miles and above [1]. These aircraft primarily serve international travel, enabling long distance flights across countries and continents. Aviation specialists can improve flight planning, operating tactics, and fuel efficiency by properly identifying and analyzing the features of short, medium, and long haul aircraft, resulting in improved passenger experiences and resource management.

As airline traffic is predicted to grow by 4% between 2022-2040 [2], the environmental pressure and pollutants near airports have become an emerging concern. According to the

Aviation Sustainability report, alternative fuel sources such as hydrogen, are predicted to reduce CO_2 emissions from 2% to 12% by 2050 [2]. Hydrogen (H_2)-combustion and fuel cell powered electric propulsion have been studied as leading alternatives for pollutant reduction [2]. The broad availability and high volumetric energy density of hydrogen make this fuel a potentially viable solution for carbon mitigation since H_2-combustion produces mainly NO_x and H_2O greenhouse gas (GHG) emissions. Such hydrogen combustion engine consists of a hydrogen powered turbofan, turboprop, or propeller that converts chemical energy into mechanical energy by combustion. Another additional alternative consists of an electric power train of a hydrogen powered SOFC hybrid that provides the necessary energy to run an electric propulsor such as a turbofan. The benefits of the use of fuel cells in aviation vehicles include a fast filling time and increased efficiency when paired with hydrogen fuel [3]. However, H_2-combustion and SOFC hybrids require large tanks to carry hydrogen in cryo-compressed liquid hydrogen (LH_2) onboard the aircraft, as well as, more complex power trains. Such LH_2 requires large storage tanks and power systems that can lead to potential range and balance compromises. Therefore, a framework methodology is needed to assess the trade-offs of implementing such alternative fuel and power sources on modern aircraft.

A comparison is performed by implementing the methodology presented in this thesis between three conventional kerosene powered aircraft, three retrofit H_2-combustion powered aircraft, and three retrofit Solid Oxide Fuel Cell (SOFC) powered aircraft. Such framework consists of a retrofit by designing liquid H_2 hydrogen tanks and a SOFC power train that meets the power and feasibility constraints for an already existing kerosene powered aircraft. These hydrogen powered technologies are not drop-in technologies, mainly due to the requirement for large tanks and changes to the power train. Thus, this framework utilizes a lifecycle emissions assessment, as well as, mission implementation costs to compare the trade-offs between implementing hydrogen, fuel cell-hydrogen hybrid, and conventional power sources. A sample study on an Embraer 170LR, Boeing 737-800, and Boeing 777-300ER is demonstrated to assess current opportunities for emissions and contrail mitigation,

as well as, performance and feasibility compromises. An analysis of the retrofitting method for a business jet was studied in a prior work presented at the AIAA SciTech conference by K.Alsamri [4], in that case, the trade-off is the removal of three passengers, along with their seats and their luggage, enabling the integration of a SOFC power train in the cabin area. The laboratory and kitchen were shifted as well forward to provide space for the SOFC power train.

This thesis intends to develop these findings by assessing and contrasting three commercial aircraft configurations: a short haul aircraft with a range of 2100 nautical miles, a medium haul aircraft with a range of 3,500 nautical miles, and a long haul aircraft with a range of 7,370 nautical miles. The main objective is to assess the trade-offs present with the commercial aircraft retrofitting process. A comprehensive analysis of the aforementioned three commercial aircraft configurations, which includes a study of their corresponding performance and emissions trade-offs, could offer beneficial information on the practicality and implications of using alternative fuel configurations. Moreover, the results of this study will be compared to the findings of the referenced publication on the retrofitted business jet. The methodology presented provides useful insight into the challenges and worries involved in integrating renewable energy sources into commercial aircraft, highlighting the trade-offs that are required to be considered carefully. The results of this study will contribute to the development of environmentally friendly aviation technologies and retrofitting methods, in addition to providing suggestions for future developments within the industry.

Aircraft share 0.04% of all annual carbon emissions [5] and they have the potential of being the first commercialized zero-emission aircraft, since a greatest 34% net energy consumption reduction is observed for hydrogen powered jets [6]. Such higher efficiency and the potential to lower emissions motivate the study of the methodology covered in the following sections.

Chapter 2

Methodology for Assessing Emissions and Performance Trade-offs

The methodology to model the alternative fuel emissions for a proposed aircraft vehicle is presented in Fig. 2.1. The inputs to the modeling framework include the aircraft characteristics, such as empty and takeoff weights, overall efficiency, and lift-to-drag ratio. In addition, the alternative fuel type is defined by the heat energy available per unit weight of fuel and mission characteristics such as range and cruising altitude. These parameters define the aircraft cruising performance in the flight profile module. Within the flight profile module, the weight of the fuel necessary to complete the mission is determined and inputted into the LH_2 tank configuration module and the emissions module. The tank configuration module models the shape, insulation, and volume of an H_2 cylindrical tank that meets the power requirements defined by the weight of the fuel. The tank volume and mass are then outputted into the center of gravity Module. This module determines the center of gravity (CG) change within the flight envelope of the aircraft by simultaneously placing the tanks in the interior layout. A tank sizing constraint is fed back into the tank configuration module if such CG requirements are not feasible for the available cargo space. The tank configu-

ration module updates the tank design and the weight of the fuel is remodeled to account for the weight of cargo removal. If such changes occur, a refueling stop is required for the same range. Such consequence is accounted for in the lifecycle emissions and cost modeling covered in detail in the following section.

Furthermore, the weight of the fuel, the mission atmospheric conditions, and the power plant for each alternative fuel type are inputted into the emissions module. Within this module, the emissions per segment are analyzed by their emission indexes, greenhouse gas emissions, and contrails. Such segment emissions are then inputted into the environmental impact module. This module implements the mentioned lifecycle assessment and cost analysis to output the trade-offs between alternative fuel power plants per mission. The details of this framework are further discussed in the following sections.

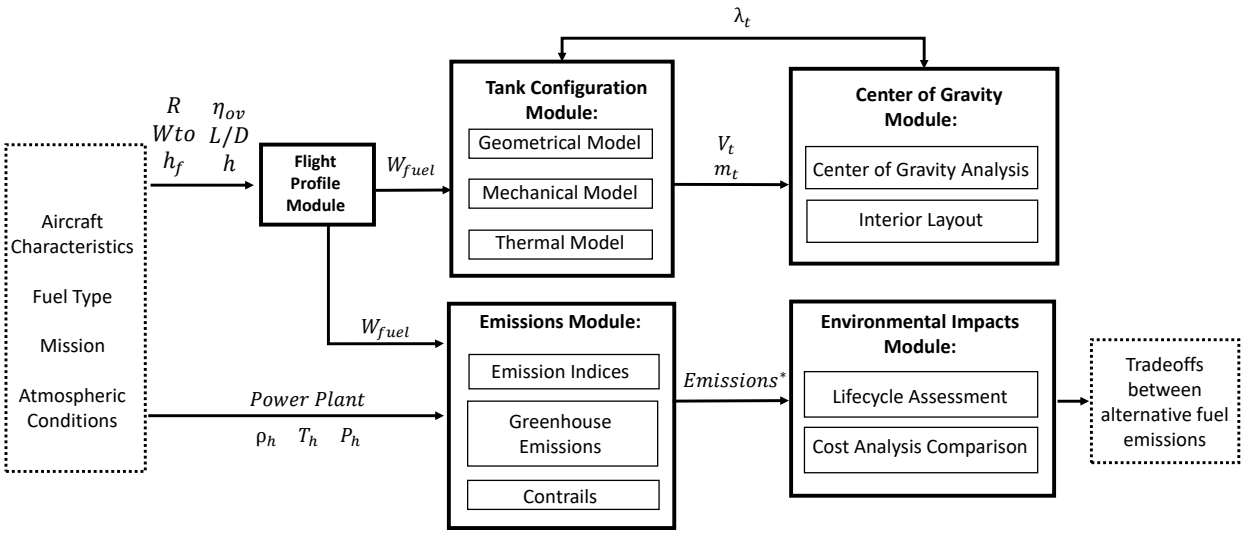

Figure 2.1: Modeling framework of the methodology to assess emissions and performance trade-offs for a retrofitted SOFC hybrid and H_2 Powered Aircraft

2.1 Flight Profile Module

The methodology presented in the previous section consists of a baseline range mission profile to compare the alternative fuel sources with a baseline kerosene gas turbine combustion flight procedure. A constant range approach analysis is implemented in order to design an alternative fuel tank and power train that satisfies insulation, the center of gravity, and power constraints. The Breguet range equation determines the weight of the fuel required to fly the given mission for the baseline and alternative fuel sources.

Hydrogen combustion would require some changes to the design of the engines due to the different properties of hydrogen such as higher adiabatic temperature and faster flame speeds. Such changes include a smaller combustion chamber, the addition of a pump, supply pipes, control valves, and turbine systems, as seen in Fig. 2.2. In addition, a heat exchanger must also be added to heat the cryogenic hydrogen liquid fuel before combustion [7], as seen in Fig. 2.3. Cryogenic hydrogen tanks become very heavy depending on the design parameters, stored pressure, temperature, and acceptable boil-off rates. Fortunately for aircraft applications, less insulation is required for short periods of flight at a relatively high boil-off rate. Design choices of a number of tanks and storage locations affect the final mass and volume of the hydrogen storage system. The high gravimetric energy density of hydrogen of a 120 MJ/kg is favorable since mass reduction is critical during flight. Hydrogen needs to be stored at its critical temperature and pressure of 33.15 Kelvin and 188.55 psi. However, the main challenge in aviation lies in the mass and volume that such cryogenic tanks occupy. Hydrogen density varies between a low of 0.08375 kg/m^3 in gaseous form and a high of 81 kg/m^3 in cryo-compressed liquid form [8]. Such densities are low when compared to the densities of kerosene variation from a low of 775 kg/m^3 to a high of 840 kg/m^3. The aforementioned hydrogen combustion system replaces the conventional turbofan for the H_2-combustion powered aircraft studied in this thesis.

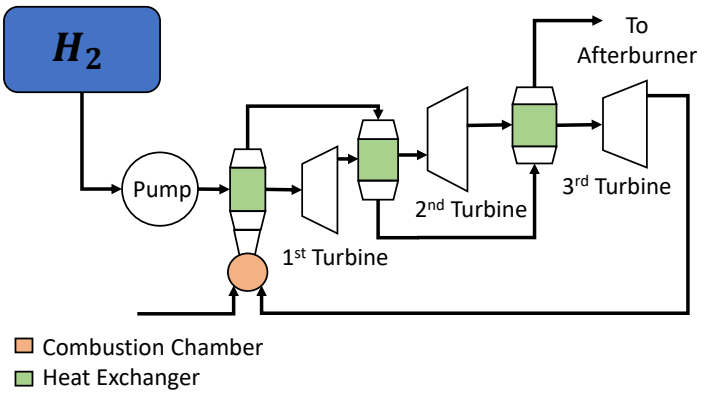

Figure 2.2: Design changes to the engine due to the different properties of hydrogen

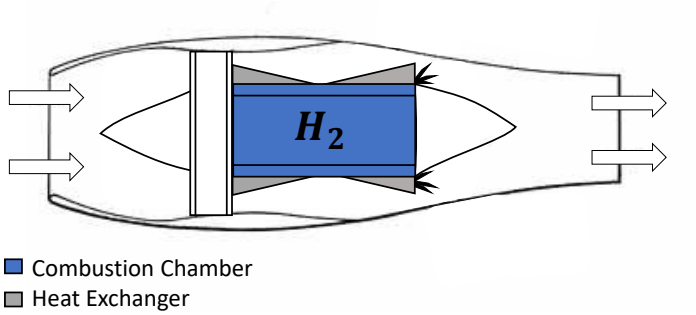

Figure 2.3: Addition of a heat exchanger for the cryogenic liquid fuel combustion

Another alternative SOFC hybrid power plant configuration is evaluated for a constant range mission. Such SOFC hybrid includes a battery and cryogenic LH_2 tanks to provide electrical power with zero emissions. Proton exchange membrane fuel cells (PEMFC) and SOFC advantages include independent power and energy scaling at efficiencies up to 60%. Unfortunately, fuel cells lose efficiency with altitude due to lower atmospheric pressure. Hence for aircraft applications, a hybrid SOFC gas-turbine system can convert fuel cell waste heat to electric power and pressurize a fuel cell [9]. The overall power system efficiency has been shown to provide slightly higher efficiencies in the range of 10% to 20% approximately for a conventional aircraft. For the SOFC hybrid, the power trains of this system consist of a gas turbine, heat exchangers, a compressor, a generator, a battery, and a LH_2 tank. The power train designed in this methodology for the SOFC hybrid for medium range and long range can be seen in Fig. 2.4. Power assumptions of the fuel cell, battery, and motor-specific

densities are assumed according to state of art (SOA) technology that can be commercially available [10]. The SOFC has gravimetric and volumetric power densities of 2.5 kW/kg and 7.5 kW/kg respectively, as determined by NASA Glen Research Center [11]. The SOFC hybrid designed by NASA has five and seven times higher gravimetric and volumetric power densities than the state-of-the-art commercially available designs. The fuel cell and motor-specific densities are found in more advanced research to be 4.0 kW/kg and 10.0 kW/kg [12]. In addition, the hybrid power train assumptions are shown in Table 2.1 where super-conducting motors and lithium-ion batteries are used. The fuel cell is assumed to power the throttle cruise at 75% power of the total energy required for this mission. The remaining 25% of power is assumed to emerge from the battery during non-cruise flight segments.

Table 2.1: Power train for SOFC hybrid

Parameters	Values
SOFC (kW/kg)(SOFC SOA)	2.5
SOFC (kW/L)	7.5
SOFC Exit Temperature ($°C$)	944
Motor Density (kW/kg)	7.064
Battery V Density (kWh/L)	0.76
Battery G Density (kW/kg)	0.35
GT-SOFC Cycle Efficiency (%)	70
GT V Density (kg/m^3)	8000
GT G Density (kWe/kg)	4.4
Motor Density (kW/kg)	7.06
Cryo-cooler Density (kg/kW)	3
Gas Turbine Power (kW)	
Short Haul	2,029
Medium Haul	4,386
Long Haul	17,524

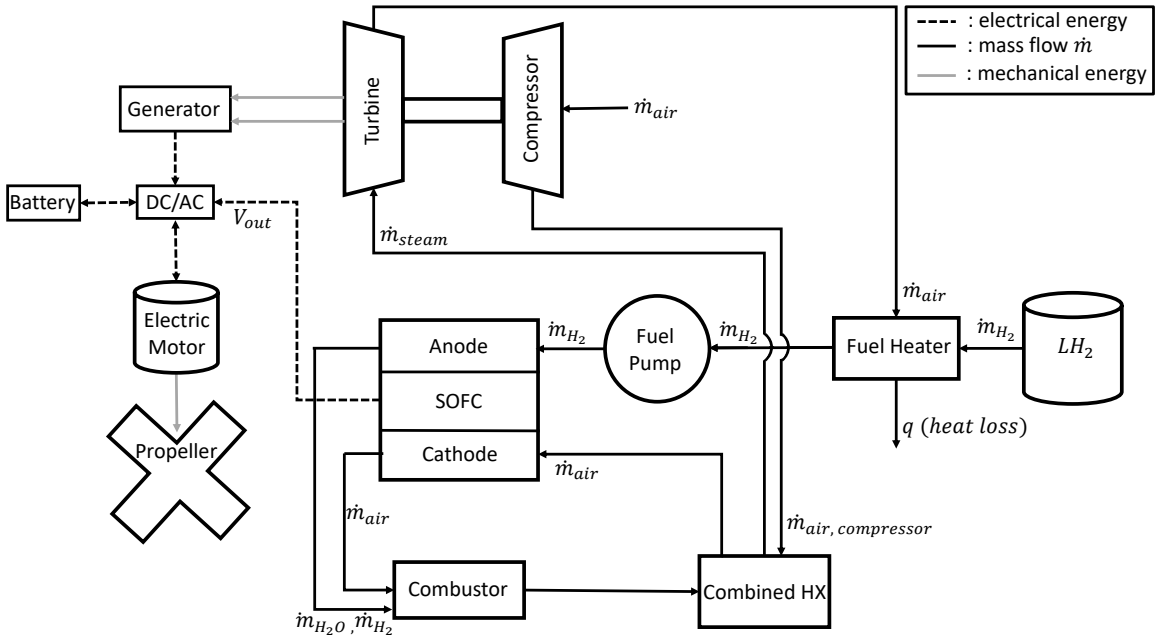

Figure 2.4: Power train SOFC hybrid for short, medium and long haul aircraft designed for fuel cell hybrid

The SOFC hybrid power train system consists of multiple components such as an electric motor, the SOFC, a generator a pump, a cryogenic tank, and other components seen in Fig. 2.4. The cryogenic tank stores liquid hydrogen fuel which vaporizes once vented from the tank. The hydrogen is then heated in a heat exchanger (HX) that acts as a fuel heater. The HX recycles heat that exits the turbine, and a fuel pump pressurizes the H_2 that is inserted the anode. Oxidation reactions occur within the anode and compressed air from the compressor is then heated in the combined HX. Such air then inlets into the cathode where the reduction reactions occur. Compressed air flow helps maintain and increase the fuel cell performance at flight altitude. The turbine is utilized to power the compressor and generator while the generator produces electricity that can be stored in the battery or used for propulsion in the electric motor.

The aforementioned H_2-combustion and SOFC hybrid system are utilized to power the constant range from the baseline kerosene flight procedure. The Breguet range equation heat energy available per unit weight accounts for such changes within this module and results in

the fuel weight outputted into the tank module. Three sample implementation cases of this methodology for both H_2-combustion and SOFC hybrid systems are performed on the three aircraft configurations in Chapter 3.

2.1.1 Tank Configuration Module

Given the design fuel weight from the previous module, tanks are modeled for a retrofitted aircraft in the tank configuration module. The design of such tanks follow the approach in Fig. 2.5. The tank module evaluates geometrical, material and thermal models that serve as feasible variables within the design space. Such tank modeling is governed by equations 2.1 to 2.9.

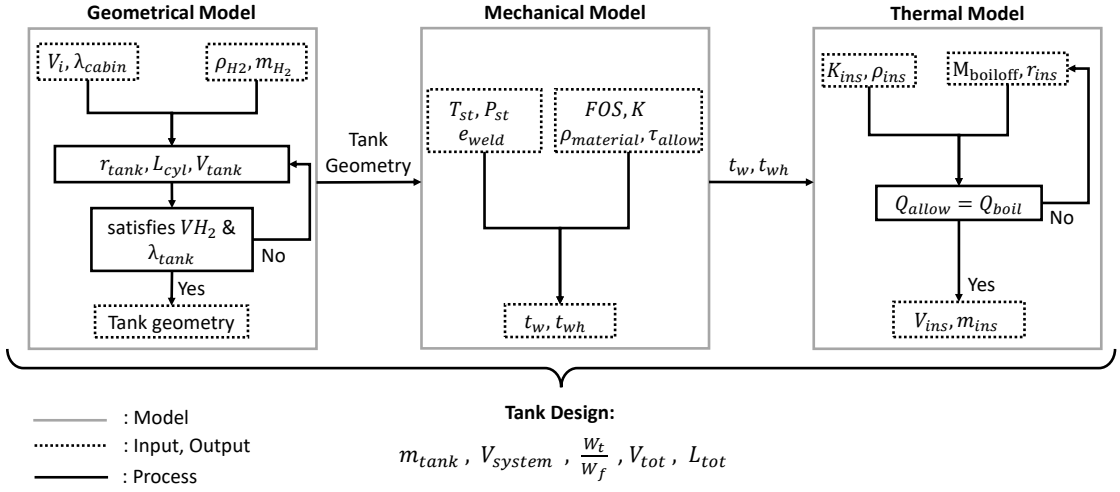

Figure 2.5: Tank configuration module flowchart [13]

Geometrical Model

The geometrical model defines the tank geometry and volume of storage required for power constraints. The tank geometry is defined as cylindrical with hemispherical ends, as hemispherical heads provide the best pressure distribution and are widely used for pressurized

vessels [14]. The excess Volume V_i is defined to be 7.2% to maintain constant pressure during boil-off with equations 2.1, 2.2 and 2.3. The volume of the capsule is delimited by a tank wall and a hemispherical insulation wall. The thickness of the wall is modeled through equations 2.4 and 2.4, where P_{des} is the pressure at which the hydrogen is stored, σ_a is the tensile strength of the material chosen, e_w is weld efficiency. Equation 2.5 models the thickness of a cylindrical tank with hemispherical ends.

$$V_t = \frac{M_{H_2}(1 + V_i)}{\rho_{LH_2}} \tag{2.1}$$

$$V_t = \frac{4 \cdot \pi r^3}{3} + r^2 \pi L \tag{2.2}$$

$$m_{filledcapsule} = \rho \pi r_1^2 (L_1 - \frac{2}{3} r_1) \tag{2.3}$$

$$t_w = \frac{P_{des} \cdot d_o}{2 \cdot \tau_a llow \cdot e_w + (0.8 \cdot P_{des})} \tag{2.4}$$

$$t_{wh} = \frac{P_{des} \cdot d_o \cdot K}{2 \cdot \tau_{allow} \cdot e_w + (2 \cdot P_{des} \cdot (K - 0.1))} \tag{2.5}$$

$$K = \frac{1}{6}(2 + \frac{d}{d_1}) \tag{2.6}$$

Mechanical Model

The geometry outputted along with material choices defines the thickness of the tank walls in the mechanical model. The choice of material for the tank walls is Aluminum (4.4 % Cu) 2014-T6 and evacuated aluminum foil separated with fluffy glass mats for insulation, as suggested by [15]. The factor of safety (FOS) for the chosen material is set to 1.3 which is within a reasonable engineering margin. The weight of the cryogenic tanks is usually within 15% to 30% of the LH_2 weight and can reach less than 15% with low enough hydrogen vaporization rates [14]. The inner vessel is placed within a vacuum with the defined geometrical thickness and passed into the thermal module to set the insulation thickness.

Thermal Model

The thermal model designs the wall insulation thickness by defining the material, acceptable boil-off rate, and consequently acceptable rate of heat transfer modeled by equations 2.7 to 2.9. In addition, the insulation layer is defined by an acceptable boil-off rate of 0.1% per hour as suggested by D. Verstraete [14]. This design's high boil-off rate minimizes insulation and reduces cost and mass. This methodology sets for 20% of the stored hydrogen to be vented per hour with a 288.15 Kelvin outer surface temperature. Such temperature maximizes range and flight time. The inner vessel is placed within a vacuum with the defined geometrical thickness and insulation to define the tank sizing constraint λ_{tanks}, as seen in Fig. 2.6. This constraint is then outputted into the center of gravity (CG) module.

$$N_{UD} = \left[0.60 + 0.287 \frac{Re_d^{\frac{1}{6}}}{\left[1 + (\frac{0.559}{Pr})^{\frac{9}{16}}\right]^{\frac{8}{27}}} \right]^2 \tag{2.7}$$

$$Q = \dot{m} \times hfg \tag{2.8}$$

$$Q = Q_{cylinder} + Q_{sphere} = \frac{2\pi Lk(T_o - T_i)}{ln(r_1 \cdot r_2)} + \frac{4\pi r_1 \cdot r_2 K(T_1 - T_2)}{r_2 - r_1} \tag{2.9}$$

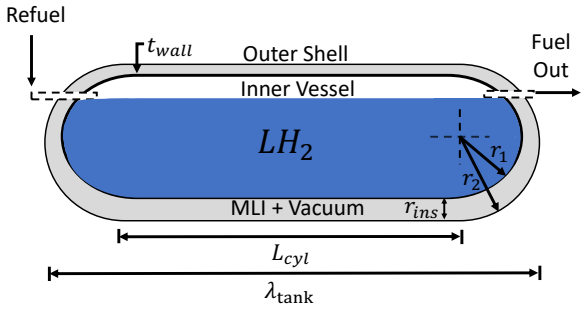

Figure 2.6: H_2 Cryogenic Tank geometry definition

2.1.2 Center of Gravity Model

Center of Gravity

A weight and balance analysis evaluates the feasibility of the tank design outputted from the tank configuration module. The changes in CG location from the operational limits of the retrofitted conventional kerosene powered aircraft are modeled from already existing

FAA-approved operational envelopes for short, medium, and long haul aircraft respectively.

Assuming the CG lies at 25 percent Mean Aerodynamic Chord (MAC) in the existing weight and balance diagrams, the change in CG is determined with the shifted weight and potential moment arm, as suggested by the FAA weight and balance handbook [16]. Such moment arm is simultaneously obtained in the interior layout of the aircraft within this module. The weight per passenger is estimated to be 180 lbs and luggage 50 lbs, as suggested by Shevell [17]. The change in weight from each alternative retrofitted fuel configuration is obtained by summing all changes in moments from either removing cargo or adding a tank, among others.

Interior Layout

Simultaneously within the center of gravity module, a potential change in the moment arm is obtained from an interior layout map of the existing aircraft. Three sample case interior layouts for short, medium, and long haul aircraft are used in Chapter 3, to obtain the dimensions of the interior, the baggage compartment, and the overall aircraft specifications for Embraer 170LR [18], Boeing 737-800 [19], and Boeing 777-300ER [20]. Such dimensions are used to evaluate and constrain the size of the tanks by placing them in a position that results in a feasible CG within the aforementioned envelope limits. After the feasible tank sizing constraints are reached in the tank configuration module, the final weight of the fuel is inputted into the emissions module. Such weight of the fuel will account for cargo weight removal in case they need to be removed to make room for the cryogenic LH_2 tanks.

2.1.3 Emissions Module

The analysis for the emissions of kerosene combustion compared to the retrofitted H_2-combustion and SOFC Hybrid system powered aircraft is modeled by inputting such power plants for the propulsive systems, and the atmospheric conditions into the emissions module. Within the emissions module, the aircraft's greenhouse emissions are determined per segment for a single flight and are dependent upon the engine type and engine thrust load. The emissions analyzed for combustion of kerosene assume complete combustion emits CO_2 and H_2O while incomplete combustion emits CO, NO_x, SO_x and HC. The emissions analyzed for H_2-combustion assume H_2O is emitted for complete combustion while incomplete combustion mainly results in NO_x with no CO, HC or SO_x emissions. However, hydrogen leaked or vented into the atmosphere still can be an emission concern [21]. The SOFC hybrid is also responsible for H_2O and NO_x emissions respectively due to the use of H_2 fuel. The details of this analysis are presented in the following sections.

Emissions Indices

The International Civil Aviation Organization (ICAO) Engine Emissions Databank (EED) is utilized to obtain the Emission Indices (EI) for the non-cruise portions of flight for kerosene powered aircraft. The cruise incomplete combustion EI of HC, and CO are taken at an average of 0.4 g/kg and 0.6 g/kg respectively, as presented by Schumann [9]. This analysis neglects SO_x emissions since the ICAO databank does not include data for the SO_x EIs. This thesis focuses on the main emissions that are in common with the three technologies that are investigated. Typically NO_x EI production ranges between 12 to 16 g/kg as supported by Schumann [9]. The EI of NO_x is dependent upon the engine design flame temperature. However, such design details are not taken into account in this analysis since a mid-value between a maximum and minimum of 14 g/kg is taken for the cruise portion of the flight. For the

purpose of comparison, the EI for pure hydrogen combustion is utilized since pure kerosene combustion is also assumed. More recent research has been able to reduce the EI_{NO_x} to 4.3 g/kg, as well as, determine a 90% reduction of NO_x emissions when compared to kerosene combustion [22],[23]. Such technologies include water injection to reduce temperatures and thus reduce thermal NO_x. Nevertheless, these technologies are harder to implement on flight compared to ground turbines since the stability of combustion is prioritized in the air. Moreover, the EI_{NO_x} is assumed to be also at 14 g/kg in the SOFC hybrid for the consistency of all technologies analyzed. The NO_x emissions in the SOFC hybrid are not coming from the fuel cell but as a result of a hydrogen combustor/micro gas turbine system that operates at high temperatures. For the kerosene combustion emissions, the composition of the fuel can also affect H_2O and CO_2 emissions since a higher H/C ratio produces more water and lower CO_2. The EI of CO_2 is modeled by accounting for the percentage of carbon in the fuel, the molar mass of CO_2, and the molar mass of carbon resulting in 3.15 kg/kg respectively. The EI of H_2O is also obtained which is 1.25 kg/kg following the same process.

Emissions

The CO_2 and H_2O emissions of kerosene are compared to the retrofitted H_2-combustion and SOFC Hybrid system powered aircraft. Such an emissions model assumes a constant percent thrust per segment and a constant aircraft Thrust-specific fuel consumption (TSFC). Each segment emission is modeled by dividing the flight profile into the segments seen in Table 2.2. The thrust per engine is taken at 100% for takeoff, 85% for climb, 30% for approach, and 7% for descent and idle, as suggested by the ICAO standard landing and takeoff cycle regulations [24]. The time to climb as referenced by the Embraer specifications pamphlet is 16 minutes [18]. Although Taxi/Idle time varies by airport, an average value of 23 minutes is assumed for this analysis. For the cruise portion of the flight, equation 2.10 models the mass fuel burned to obtain the total emissions of CO_2, H_2O, CO, HC, and NO_x. A sample of

implementing this methodology for modeling emissions is demonstrated in detail in Section 3.1.

$$E_x = m \cdot EI(X) \tag{2.10}$$

Table 2.2: Assumed flight profile segments medium, short, and long haul [25][26]

Segment	Duration (min)	Thrust (%)
Takeoff	0.7	100
Climb	16	85
Descent	25	7
Approach	4	30
Taxi/Idle	23	7

Contrails

The likelihood of contrail formation using kerosene, H_2-combustion fuel, and a SOFC hybrid-powered aircraft is modeled using mass and energy balances to determine the mixing line slope G. An aircraft exhaust plume mixes isobarically with exhaust air and can lead to the possibility of contrail formation [24]. Contrails may form by the mixing of hot and humid air with cold ambient air below a critical temperature threshold, as defined by the "Schmidt-Appleman" criterion [27], which is modeled by equation 2.11.

$$G = \frac{Pa \cdot EI(H_2O) \cdot Cp_{air}}{\epsilon_{H_2O} \cdot LHV_{fuel} \cdot (1 - \eta_{overall})} \tag{2.11}$$

Such contrails are evaluated since they can increase the overall warming effect due to trapped heat in the atmosphere and affect cooling from reflected sunlight [28]. The overall efficiency of the aircraft is assumed constant for all three configurations. The H_2-combustion and SOFC hybrid are expected to have a shallower slope than kerosene due to a higher LHV_{fuel} value of 120 MJ/kg. Such value is higher when compared to the conventional lower 43 MJ/kg kerosene LHV_{fuel}, as seen in Section 3.1. However, an increase in the mixing slope G arises from the higher EI of H_2O when using liquid hydrogen fuel. The persistence of contrails is not explored due to the location dependence of atmospheric conditions at every point of the duration of a single flight.

2.1.4 Environmental Impacts Module

Lifecycle Assessment

A complete lifecycle analysis (LCA) of CO_2 evaluates the environmental effects of the medium, short, and long haul conventional kerosene powered aircraft, medium, short, and long haul retrofit H_2-combustion aircraft, and medium, short, and long haul retrofit SOFC hybrid powered aircraft. This lifecycle analysis takes into account two separate cases. Case's (i) flights are restricted to carry-on luggage keeping the same number of passengers and a fixed range for each haul as in the conventional kerosene configurations. In case (ii) the analysis focuses on a worst-case scenario in which passenger capacity is decreased by 50% to accommodate checked-in luggage in the remaining empty cabin space. Case (ii) also necessitates two flights, along with each haul's refueling stops, to fly all of the passengers matching the passenger capacity of both case (i) and conventional kerosene powered configuration. This assessment intends to give a more appropriate evaluation of the advantages and disadvantages associated with these various configurations, providing a better informed knowledge regarding the environmental implications in terms of CO_2 emissions by comparing

cases (i) and (ii). The lifecycle emissions are modeled for the various stages of fuel extraction, transport, processing, and storage sectors known as Well-to-Tank (WTT), and a combustion sector known as Tank-to-Wheel (TTW), as seen in Fig. 2.7. Such LCA evaluates the consequences of eliminating the dependency of aviation upon dwindling crude oil resources, as well as, the overall contribution of aviation to the anthropogenic greenhouse effect [29].

The carbon intensity of Jet-A fuel can vary depending on the region, the refinery, and the crude oil well. Various studies have estimated that the carbon intensity of jet fuel ranges from 85 to 95 grams of CO_2 per MJ [30]. The combustion of fuel contributes to a portion of 73 grams of CO_2e/MJ, while the rest is generated by transportation, processing, and the refinement process [30]. The Well-to-Wheel (WTW) CO_2 emissions for Jet-A fuel are modeled at 84.5 gCO_2e/MJ with an 87% in combustion emissions, as supported by Wang [31]. Finally, the complete lifecycle of kerosene WTW is found by adding WWT to TTW CO_2 emissions of kerosene and LH_2 fuel sources from the extraction of crude oil or fuel to its combustion during flight.

The WTW for both H_2-combustion and the SOFC hybrid is estimated using green and gray hydrogen. Green hydrogen refers to the hydrogen produced via renewable energy, while gray hydrogen refers to the hydrogen produced using steam methane reformation without any gene house gas (GHG) emissions capture. More than 95% of hydrogen produced today is produced using fossil fuels like natural gas and coal [32]. Meanwhile, green hydrogen requires a renewable energy-powered grid which is not yet available in many parts of the world. However, most countries have plans to reach 100% renewable grids within the next 30-50 years [32]. The LCA estimation utilizes the Greenhouse Gases, Regulated Emissions, and Energy Use in Technologies (GREET) model to estimate the transportation lifecycle emissions via a mathematical framework that accounts for various pollutants such as CO_2 [33]. In addition, green hydrogen solar electrolysis is assumed to emit 41.29 grams of CO_2e/MJ for the full lifecycle, as referenced by Al-Breiki [33]. Similarly, the gray hydrogen solar electrolysis full

lifecycle is assumed to emit 75.6 g CO_2e/MJ, as sourced by [34].

The mentioned LCA model does not include the production or life expectancy of lithium-ion batteries and the SOFC. The model is thus focused on the fuel WTW lifecycle. Although, the environmental effects of producing those components are mainly from mining, not enough current data and research are available on the lifecycle analysis of the SOFC hybrid system. TTW CO_2 emissions for all alternative fuel sources are modeled from the weight of the fuel inputted from the flight profile module as discussed in Section 2.1.3.

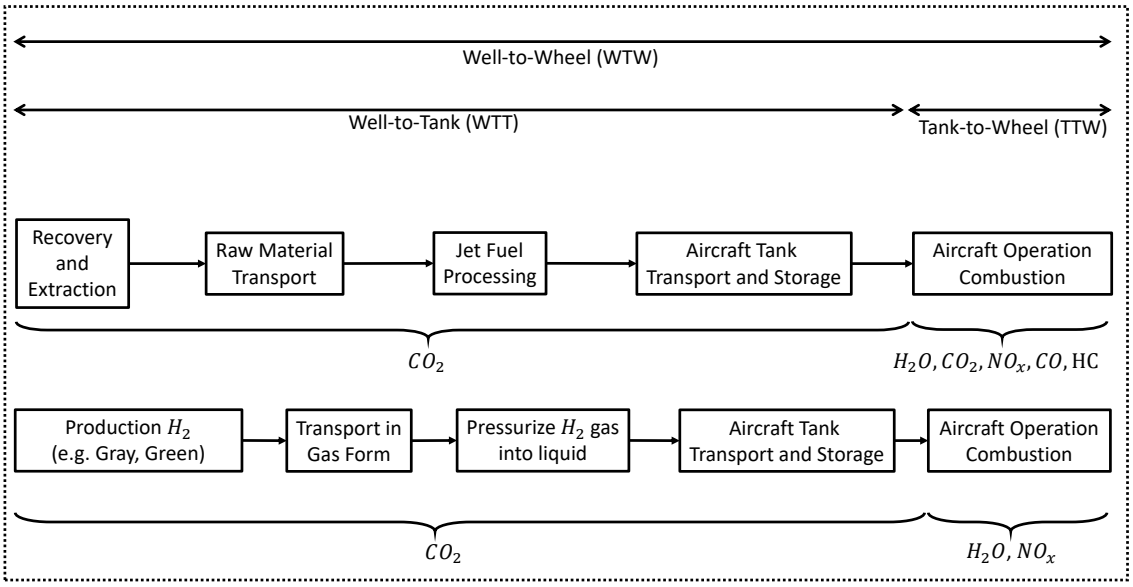

Figure 2.7: Lifecycle Assessment (LCA) boundary of Jet-A Fuel (Top) and LH_2 fuel (Bottom)

Cost Analysis

The change in fuel cost of implementing alternative fuel sources for one constant range flight profile is determined to further analyze the trade-offs of implementing a retrofit. The total fuel burned from the emissions module is utilized to model the fuel price per flight for this mission, in addition to the change in capital cost of the alternative fuel source.

The cost for kerosene is determined from the full-service average kerosene Jet-A fuel price

per gallon for the U.S. Western Pacific region for the current year. The price at the pump is assumed to already contain the production and transportation costs of kerosene. The cost of utilizing LH_2 for the proposed flight is modeled per segment in order to compare the change in fuel cost from a conventional kerosene powered flight.

The H_2-combustion change in fuel costs are estimated for both green and gray hydrogen. The cost of production for green hydrogen (electrolysis) is set to 5.5 USD/kg while the production for gray carbon capture hydrogen is taken at 1.55 USD/kg, as suggested by [35]. The cost liquefaction of both was set to 2.75 USD/kg as suggested by [36], while the cost for transportation was set to 5 USD/kg, as referenced by [37]. In addition, the cost of implementing the LH_2 cryogenic tanks designed by this methodology is determined. Such costs are estimated from cryogenic tank market prices and are taken at 34 dollars per lb of maximum LH_2 fuel weight, as suggested by Yang [38].

The SOFC hybrid cost is modeled for the purpose of comparison with LH_2 prices are determined as stated above. In addition, the stack cost at a high production volume of SOFC is determined to be 238 USD per kilowatt of energy, as suggested by Scataglini [39]. A 500 kW microturbine is assumed to be in a mid-range market price of 900 dollars per kW following the California Distributed Energy Resources Guide on Microturbines as resourced by Capehart [40]. The lithium-ion battery cost is estimated to be 135 USD per kilowatt hour for the current year as determined by [41].

Chapter 3

Methodology Demonstration for Alternative Fuel Retrofit on Short, Medium, and Long Haul Aircraft

The developed methodology in the previous section evaluates the potential to lower emissions for short, medium, and long haul aircraft by utilizing a retrofit analysis. As global commercial air travel has risen, the implementation of the aforementioned methodology on the short haul Embraer 170LR, medium haul Boeing 737-800, and long haul Boeing 777-300ER presents a potential opportunity for carbon mitigation. A summary of key mission and performance specifications for the three aforementioned aircraft is found in Table 3.1:

Table 3.1: Aircraft performance specifications [18], [19], [20]

Parameter	E170LR	B737-800	B777-300ER
Cruise Range (nmi)	2,100	3,500	7,370
Maximum Number of Passengers	76	160	350
Maximum Speed Limit (Mach)	0.80	0.82	0.87
Maximum Operating Altitude (ft)	40,000	40,000	40,000
TSFC (lbf/lbhr)	0.68	0.60	0.55

The methodology presented in Chapter 2 is utilized to model the performance and emissions of the three standard kerosene powered aircraft in order to compare the trade-offs resulting from a retrofitted H_2-combustion fuel and SOFC hybrid powered aircraft. In the flight profile module, these two alternative fuel power sources are examined for the same mission profile as the kerosene baseline procedure. The weights of the fuel required for these missions are determined for all three power plants as a function of heat energy available per unit weight of fuel, range, and other Breguet range equation parameters as seen in Section 2.1. Such weights are utilized to design the cryogenic tanks as stated in Section 2.1.1 and evaluated for feasibility in the center of gravity module, as shown in Section 2.1.2. A portion of cargo might be dropped if tank sizing volume constraints are required to power the same mission. A new fuel weight that accounts for such changes is then outputted into the emissions module. The flight emissions are then used to assess the lifecycle assessment and costs of implementing each retrofit. An overall analysis of the trade-offs in performance and emissions by a retrofit methodology is outputted.

3.1 Analysis of Results

The conventional kerosene, the H_2-combustion, and the SOFC hybrid powered retrofit aircraft are all able to power the cruise mission specifications from Table 3.1. The fuel weights obtained from the flight profile module in Section 2.1 are seen in Table 3.2:

Table 3.2: Fuel weights for cruise

Haul	Jet-A (lbs)	H_2-combustion (lbs)	SOFC (lbs)
Short	$17,404.35$	$6,719.45$	$3,938.27$
Medium	$36,961.85$	$14,270.19$	$8,891.75$
Long	$313,144.14$	$131,200.89$	$78,825.50$

The power requirements and constraints of the H_2-combustion fuel and SOFC hybrid powered aircraft follow the energy assumptions described in Section 2.1, and are seen in Table 3.3. The power rating of the electric propulsion system is defined based on the maximum takeoff velocity of the aircraft and the thrust of the conventional aircraft. The battery size is defined as providing maximum thrust for 15 minutes. Such parameters and the fuel weight are used as design constraints in the tank configuration module.

Table 3.3: Power and SOFC energy requirements

Parameters	Short Haul	Medium Haul	Long Haul
Thrust Per Engine (lbf)	14, 200	27,300	115,300
Maximum T/O Velocity (knots)	138	153	145
Engine Max Power (kW)	8,845.80	19,117	76,385
Energy Required by H_2-combustion (MJ)	214,364.56	483,988.41	4,290,562.23
Energy (kJ)(kWh)	59,545.71	134,441.23	1,191,822.84
Fuel Cell Power (75%)(kW)	6,634.32	14,337.80	57,288.48
Battery Power (25%)(kW)	2,211.44	4,779.26	19,096.16
Battery Size (kWh)	552.86	1,194.81	4,774.04
Cryocooler Maximum Power (kg/kW)	88.46	191.17	763.85

The hydrogen cryogenic tanks for the short, medium, and long haul configurations are designed with insulation and altitude pressure as added design constraints. The resulting tank materials, properties, and characteristics are detailed in the following sections of analysis of results for each configuration. The insulation design maximizes flight temperature as specified in the Thermal Model in 2.1.1. The cryogenic tanks of each configuration are then evaluated for feasibility in the center of gravity module. The following sections detail the results of implementing H_2-combustion and SOFC hybrid systems for the three configurations (short, medium, long haul).

3.1.1 Tank Design and Interior Layout

Short Haul Aircraft

The LH_2 tank design and layout results in seven cryogenic tanks each 374.02 inches in length distributed at the CG location of the cargo compartment, one with 17.72 inches radius size (shown in blue), two with 12.99 inches radius size (shown in green), and four with the radius of 4.92 inches (shown in pink) as seen in Fig. 3.2a and Fig. 3.1. It needs to be addressed that the overall tank length of the cryogenic tanks in Fig. 3.2a are designed in such a way that the CG of the aircraft does not shift while still allowing for 45% cargo space. It is chosen to constrain the length of the tanks since increasing them to their maximum potential length not only shifted the CG location and completely eliminated the cargo space, but also failed to omit the need for a refueling stop. Regardless of tank length, the H_2-combustion design requires two refueling stops to travel the full 2,100 nautical miles range, since the H_2 fuel needed to cover the entire range is 10,656.17 gallons which is close to three times greater than the total volume of the seven tanks' capacities as can be seen in Table 3.4. Consequently, the length of the cryogenic tanks is designed to ensure minimal CG movement while compromising the capability to fulfill the specified distance without refueling. Consequently, as a trade-off for using the cargo space without eliminating cabin seats to house larger radius cryogenic tanks within the cabin section, the short haul aircraft requires two refueling stops. The presence of the refueling stops necessitates further examination in Section 3.1.3 to assess how this impacts the emissions of the H_2-combustion aircraft, as well as examine the two cases presented earlier in Section 2.1.4 regarding the CO_2 emissions for the full LCA in Section 3.1.3. The complete tank dimensions and characteristics are seen in Table 3.4.

Table 3.4: Cryogenic LH_2 tanks for short haul H_2-combustion

Size	1 (Blue)	2 (Green)	4 (Pink)
r_{tank} (in)	17.72	12.99	4.92
L_{tank} (in)	374.02	374.02	374.02
V_{tot} (gal)	1,696.54	1,795.79	501.16
Insulation Thickness (in)	0.0031	0.00314	0.00315

While the H_2-combustion layout requires the removal of the forward cargo compartment, the SOFC layout however necessitates removing part of the forward and aft cargo compartment. This alteration is implemented to accommodate the LH_2 cryogenic tanks and the SOFC power train, at the cost of losing 67% cargo space. The 113.78-inch-long SOFC power train is positioned at the aircraft CG point in the SOFC layout, requiring a redesign of the LH_2 cryogenic tanks from the H_2-combustion layout. The redesigned LH_2 cryogenic tanks, each measuring 130.87 inches in length, are arranged symmetrically forward and aft of the SOFC power train. This layout allows for the change in CG for the Short Haul aircraft configuration to remain zero. The 130.87-inch-long modified LH_2 cryogenic tanks are symmetrically placed forward and aft of the SOFC power train. This setup holds the CG change for the Short Haul aircraft configuration at zero. The SOFC hybrid aircraft, similar to the H_2-combustion aircraft, requires a refueling stop. In this instance, however, only one refueling stop is necessary for covering the entire range as the amount of H_2 fuel required to cover the complete range is 6,245.66 gallons, which is two times the total amount of the 14 tanks' capacities. The presence of the refueling stop necessitates further examination in 3.1.3 to assess how this impacts the emissions of the SOFC hybrid aircraft. The complete tank dimensions and characteristics are seen in Table 3.5 as well as the dimensions for the SOFC power train in Table 3.6. The SOFC power train is shown in light blue, and the LH_2 cryogenic tanks are shown in blue in Fig 3.2b and a visualization of the tanks' cross-section

dimensions can be seen in Fig. 3.1 and in Table 3.5.

Table 3.5: Cryogenic LH_2 tanks for short haul SOFC hybrid combustion

Tank Size	2 (Blue)	4 (Green)	8 (Pink)
r_{tank} (in)	17.72	12.99	4.92
L_{tank} (in)	130.87	130.87	130.87
V_{tot} (gal)	1,377.39	1,423.68	380.20
Insulation Thickness (in)	0.0031	0.00314	0.00315

Table 3.6: SOFC power train for short haul SOFC hybrid combustion

SOFC	Length (in)	Width (in)	Height (in)	V_{tot} (gal)
(Light Blue)	113.78	29.52	37.01	514.87

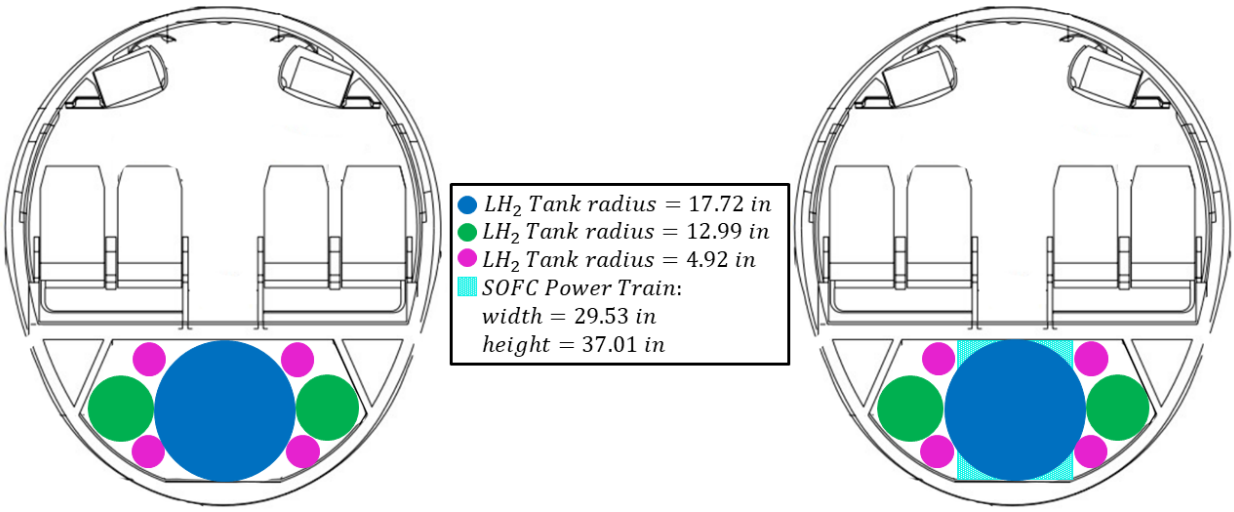

Figure 3.1: Cross section of short haul fuselage: (Left) H_2-combustion (Right) SOFC hybrid combustion

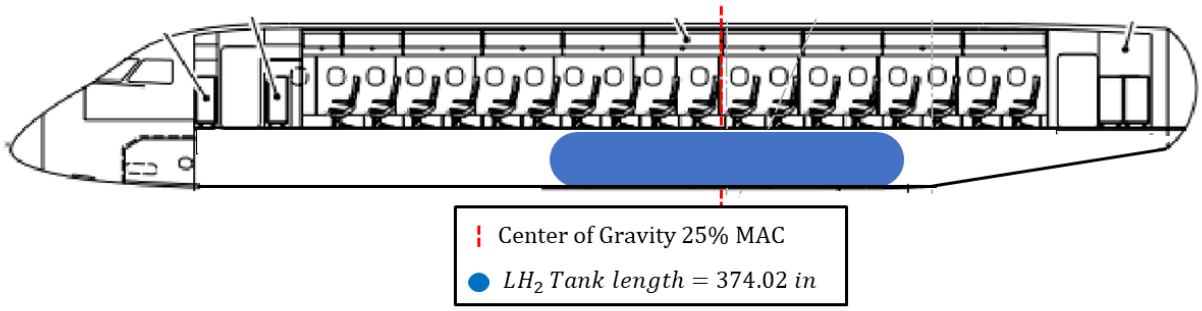

(a) H_2-combustion

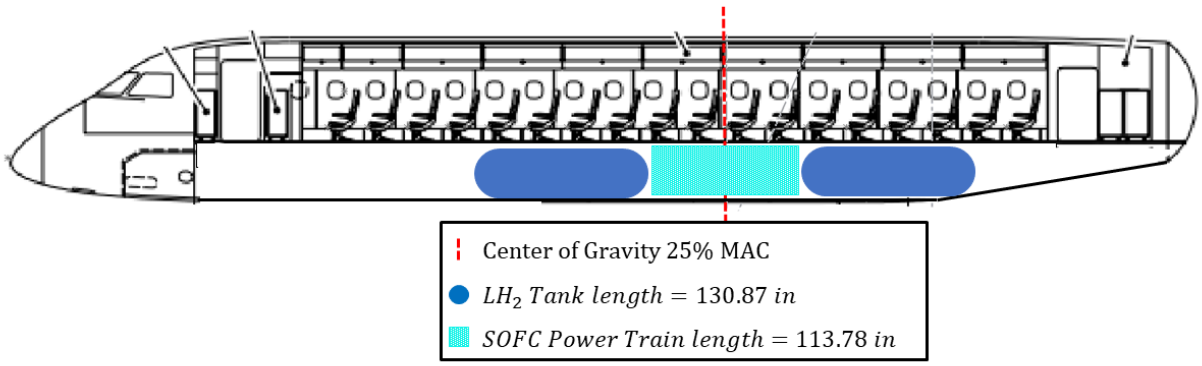

(b) SOFC hybrid

Figure 3.2: Side view layouts for short haul retrofit analysis

Medium Haul Aircraft

The medium haul LH_2 cryogenic tank design and layout results in three tanks each 708.66 inches long distributed in the CG location of the cargo compartment, one of the 20.66 inches radius size (shown in blue), and two of 15.75 inches radius size (shown in green) as seen in Fig. 3.4a and Fig. 3.1. Similarly to the short haul's configuration, the overall tank length of the cryogenic tanks in Fig. 3.4a are designed in such a way that the CG of the aircraft does not shift. It is chosen to constrain the length of the tanks since increasing them to their maximum potential length not only shifted the CG location and completely eliminated the cargo space, but also failed to omit the need for a refueling stop. Regardless of tank length,

the H_2-combustion design requires two refueling stops to travel the full 3,500 nautical miles range, since the H_2 fuel needed to cover the entire range is 22,630.30 gallons which is close to three times greater than the total volume of the three tanks' capacities (9,194.83 gal) as can be seen in Table 3.7. Consequently, the length of the cryogenic tanks is designed to ensure minimal CG movement while compromising the capability to fulfill the specified distance without refueling. Consequently, as a trade-off for using the cargo space without eliminating cabin seats to house larger radius cryogenic tanks within the cabin section, the medium haul aircraft requires two refueling stops. The presence of the refueling stops necessitates further examination in Section 3.1.3 to assess how this impacts the emissions of the H_2-combustion aircraft, as well as examine the two cases presented earlier in Section 2.1.4 regarding the CO_2 emissions for the full LCA in Section 3.1.3. The complete tank dimensions and characteristics are seen in Table 3.7.

Table 3.7: Cryogenic LH_2 tanks for medium haul H_2-combustion

Size	1 (Blue)	2 (Green)
r_{tank} (in)	20.67	15.75
L_{tank} (in)	708.66	708.66
V_{tot} (gal)	4,275.36	4,919.46
Insulation Thickness (in)	0.0031	0.00314

While the H_2-combustion layout requires the removal of the forward cargo compartment, the SOFC layout however necessitates removing part of the forward and aft cargo compartment. This alteration is implemented to accommodate the LH_2 cryogenic tanks and the SOFC power train, at the cost of losing 70% cargo space. The 121.26-inch-long SOFC power train is positioned at the aircraft CG point in the SOFC layout, requiring a redesign of the LH_2 cryogenic tanks from the H_2-combustion layout. The redesigned LH_2 cryogenic tanks, each measuring 295.28 inches in length, are arranged symmetrically forward and aft

of the SOFC power train. This layout allows for the change in CG for the medium haul aircraft configuration to remain zero. The 295.28-inch-long modified LH_2 cryogenic tanks are symmetrically placed forward and aft of the SOFC power train. This setup holds the CG change for the medium haul aircraft configuration at zero. The SOFC hybrid aircraft, similar to the H_2-combustion aircraft, requires a refueling stop. In this instance, however, only one refueling stop is necessary for covering the entire range as the amount of H_2 fuel required to cover the complete range is 14,100.98 gallons, which is two times the total amount of the six tanks' capacities (8,014.24 gal). The presence of the refueling stop necessitates further examination in 3.1.3 to assess how this impacts the emissions of the SOFC hybrid aircraft. The complete tank dimensions and characteristics are seen in Table 3.8 as well as the dimensions for the SOFC power train in Table 3.9. The SOFC power train is shown in light blue, and the LH_2 cryogenic tanks are shown in blue in Fig 3.4b and a visualization of the tanks' cross-section dimensions can be seen in Fig. 3.3 and in Table 3.8.

Table 3.8: Cryogenic LH_2 tanks for medium haul SOFC hybrid combustion

Tank Size	2 (Blue)	4 (Green)
r_{tank} (in)	20.67	15.75
L_{tank} (in)	295.28	295.28
V_{tot} (gal)	3,749.55	4,264.69
Insulation Thickness (in)	0.0031	0.00314

Table 3.9: SOFC power train for medium haul SOFC hybrid combustion

SOFC	Length (in)	Width (in)	Height (in)	V_{tot} (gal)
(Light Blue)	121.26	48.03	44.09	1,112.69

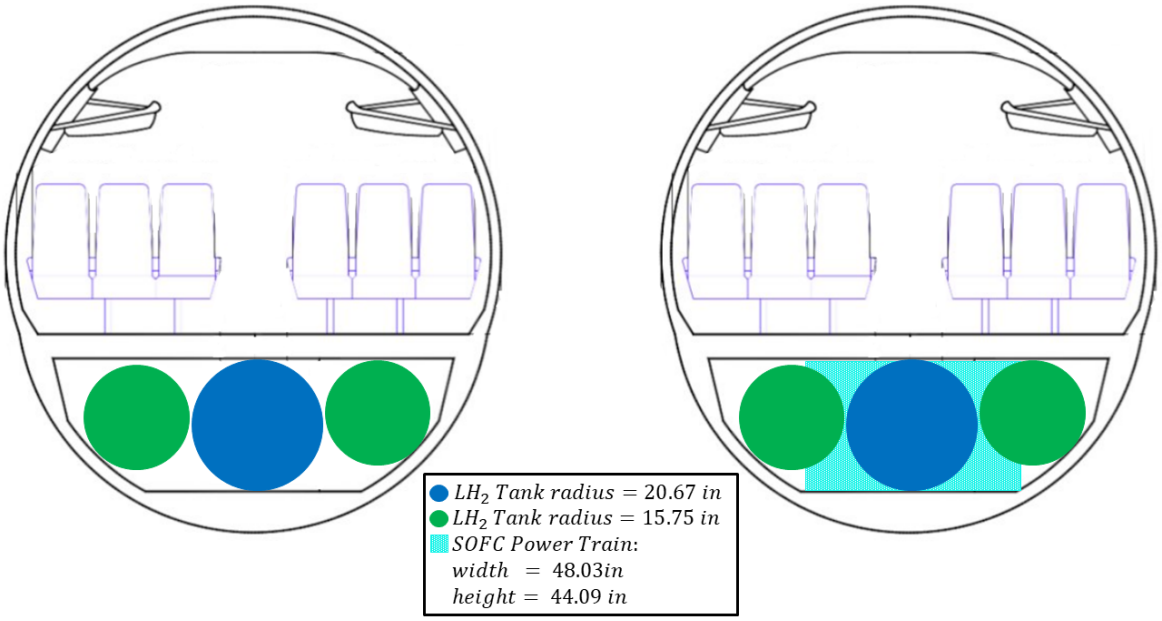

Figure 3.3: Cross section of medium haul fuselage: (Left) H_2-combustion (Right) SOFC hybrid combustion

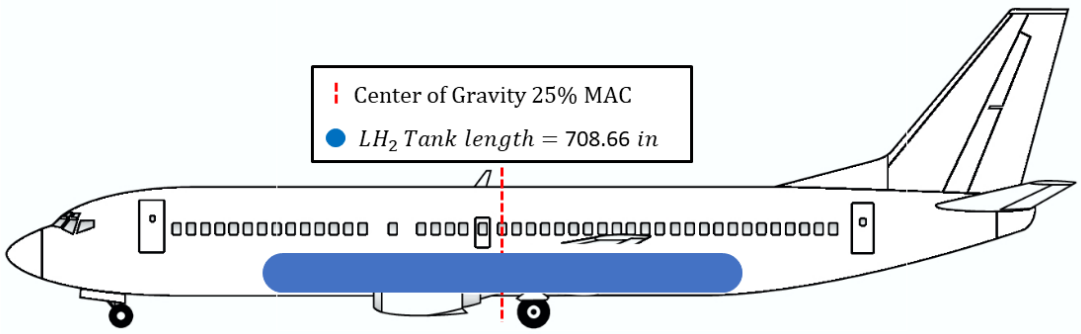

(a) H_2-combustion

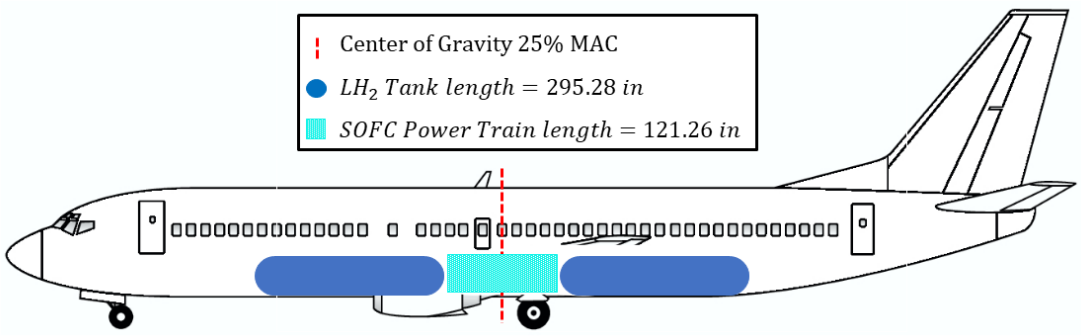

(b) SOFC hybrid

Figure 3.4: Side view layouts for medium haul retrofit analysis

Long Haul Aircraft

Lastly, the long haul layout resulted in seven 1,574.8 inches long LH_2 tanks also distributed at the CG location of the aircraft, one with 33.46 inches radius size (shown in blue), two with 27.56 inches radius size (shown in green), two with the radius of 9.84 inches (shown in pink), and two with the radius of 7.87 inches (shown in orange) as seen in Fig. 3.6a and Fig. 3.5. It is chosen for this configuration as well to constrain the length of the tanks since increasing them to their maximum potential length not only shifted the CG location and completely eliminated the cargo space, but also failed to omit the need for a refueling stop. Regardless of tank length, the H_2-combustion design requires three refueling stops to travel the full 7,370 nautical miles range, since the H_2 fuel needed to cover the entire range is 208,064.55 gallons which is close to three times greater than the total volume of the seven tanks' capacities (64,722.20 gal) as can be seen in Table 3.10. Consequently, the length of the cryogenic tanks is designed to ensure minimal CG movement while compromising the capability to fulfill the specified distance without refueling. As a trade-off for using the cargo space without eliminating cabin seats to house larger radius cryogenic tanks within the cabin section, the long haul aircraft requires three refueling stops. The presence of the refueling stops necessitates further examination in Section 3.1.3 to assess how this impacts the emissions of the H_2-combustion aircraft, as well as examine the two cases presented earlier in Section 2.1.4 regarding the CO_2 emissions for the full LCA in Section 3.1.3. The complete tank dimensions and characteristics are seen in Table 3.10.

Table 3.10: Cryogenic LH_2 tanks long haul H_2-combustion

Size	1 (Blue)	2 (Green)	2 (Pink)	2 (Orange)
r_{tank} (in)	33.46	27.56	9.84	7.87
L_{tank} (in)	1,574.80	1,574.80	1,574.80	1,574.80
V_{tot} (gal)	24,568.00	33,285.70	4,226.75	2,641.72
Insulation Thickness (in)	0.0031	0.00314	0.00315	0.00315

While the H_2-combustion layout requires the removal of the cargo compartment, the SOFC layout however necessitates removing part of the forward and aft cargo compartment. This alteration is implemented to accommodate the LH_2 cryogenic tanks and the SOFC power train, at the cost of losing 76% cargo space. The 116.53-inch-long SOFC power train is positioned at the aircraft CG point in the SOFC layout, requiring a redesign of the LH_2 cryogenic tanks from the H_2-combustion layout. The redesigned LH_2 cryogenic tanks, each measuring 590.55 inches in length, are arranged symmetrically forward and aft of the SOFC power train. This layout allows for the change in CG for the long haul aircraft configuration to remain zero. The 590.55-inch-long modified LH_2 cryogenic tanks are symmetrically placed forward and aft of the SOFC power train. This setup holds the CG change for the long haul aircraft configuration at zero. The SOFC hybrid aircraft, similar to the H_2-combustion aircraft, requires a refueling stop. In this instance, however, only two refueling stops are necessary for covering the entire range as the amount of H_2 fuel required to cover the complete range is 125,006.22 gallons, which is three times the total amount of the 14 tanks' capacities (50,446.30 gal). The presence of the refueling stop necessitates further examination in 3.1.3 to assess how this impacts the emissions of the SOFC hybrid aircraft. The complete tank dimensions and characteristics are seen in Table 3.11 as well as the dimensions for the SOFC power train in Table 3.12. The SOFC power train is shown in light blue, and the LH_2 cryogenic tanks are shown in blue in Fig 3.6b and a visualization of the tanks' cross-section

dimensions can be seen in Fig. 3.1 and in Table 3.11.

Table 3.11: Cryogenic LH_2 tanks for long haul SOFC hybrid combustion

Size	2 (Blue)	4 (Green)	4 (Pink)	4 (Orange)
r_{tank} (in)	33.46	27.56	9.84	7.87
L_{tank} (in)	590.55	590.55	590.55	590.55
V_{tot} (gal)	19,337.92	25,904.71	3,179.80	2,026.20
Insulation Thickness (in)	0.0031	0.00314	0.00315	0.00315

Table 3.12: SOFC power train for long haul SOFC hybrid combustion

SOFC	Length (in)	Width (in)	Height (in)	V_{tot} (gal)
(Light Blue)	116.53	122.05	69.69	4,446.28

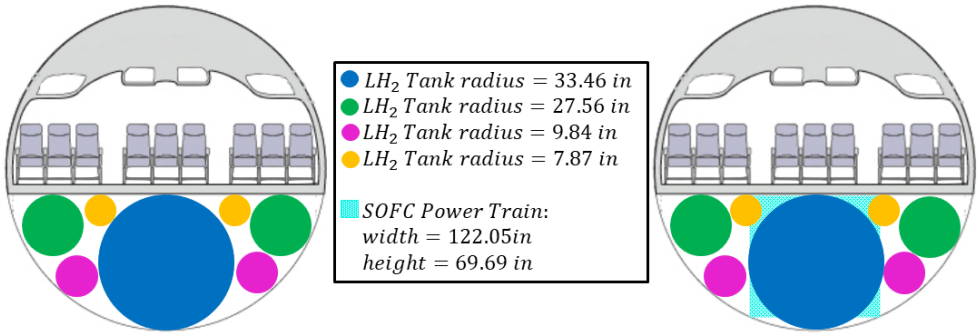

Figure 3.5: Cross section of long haul fuselage: (Left) H_2-combustion (Right) SOFC hybrid combustion

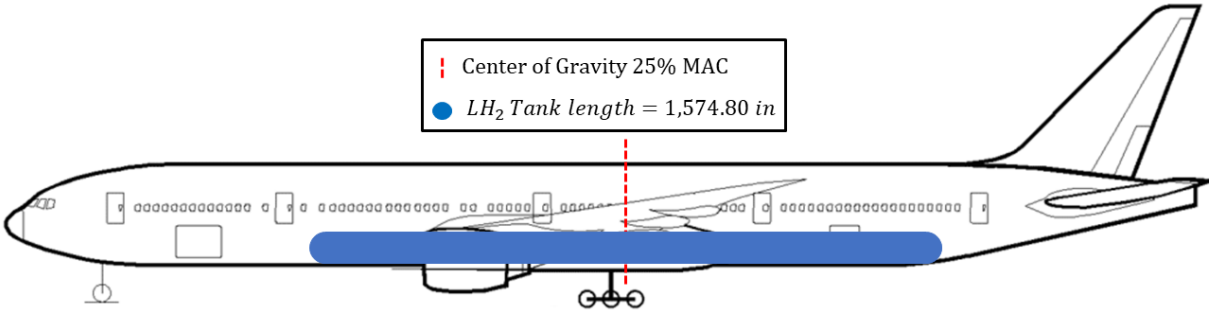

(a) H_2-combustion

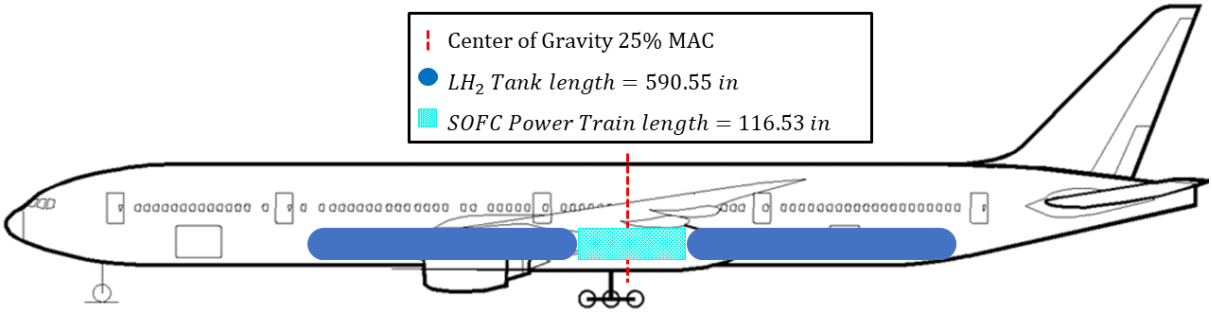

(b) SOFC hybrid

Figure 3.6: Side view layouts for long haul retrofit analysis

The H_2-combustion layout required the removal of the cargo compartment and the SOFC layout required the removal of a portion of the forward and aft cargo compartment in order to fit the cryogenic LH_2 tanks as well as the SOFC power train. The H_2-combustion layout of each aircraft is shown in Figs. 3.2a, 3.4a, and 3.6a. However, the SOFC power train is placed at the CG location of each aircraft, this required the modification of the cryogenic LH_2 tanks from the H_2-combustion layout. The modified LH_2 tanks are then positioned forward and aft of the SOFC power train symmetrically, such that the change in CG of each aircraft configuration maintains at zero. The SOFC power trains are shown in light blue, and the LH_2 tanks are shown in blue for the short, medium, and long haul layouts in Figs. 3.2b, 3.4b, and 3.6b respectively.

Refuel Stops

Table 3.13 below, includes all the necessary refuel stops for all three hauls that are analyzed in this section 3.1.1. It is crucial to note how many refuel stops the long haul configuration requires for both cases. The worst scenario is in case (ii) for H_2-combustion in which the aircraft is required to make a total of six refuel stops, by taking into account that in case (ii) the number of refuel stops doubles since the objective of the analysis is to transport the same amount of passengers for all configurations. This result inspires a further analysis regarding the cost of all the hauls' cases which is analyzed further in the following section 3.1.2.

Table 3.13: Required refuel stops for fixed range

Haul	Case	H_2-combustion	H_2 SOFC
Short & Medium	(i)	2	1
	(ii)	4	2
Long	(i)	3	2
	(ii)	6	4

3.1.2 Cost for Short, Medium, and Long Haul Configurations

Fuel Cost

From the economic point of view, significant fuel cost changes for cases (i) and (ii) result from replacing kerosene with alternative fuel sources, with no fuel cost reduction in any of the retrofit configurations, as seen in Table 3.14. The reason for these high cost changes comes directly from all the refuel stops that are required for each configuration to complete the fixed range in case (i) and fly the same amount of passengers as in the conventional powered aircraft in case (ii). The cost of green H_2-combustion for all three hauls is 28.46%

higher than gray H_2 due to the increased cost of green H_2 production for cases (i) and (ii). As for the gray H_2-combustion in case (i) the fuel cost is 34.88% higher than that of kerosene. Case (ii) for all the retrofit configurations is 50% higher at fuel cost since they require double the fuel compared to case (i). Furthermore, case (ii) for SOFC green H_2 is 80.58% higher at cost and H_2 gray is 67.44% more expensive when compared to the conventional kerosene aircraft.

The SOFC gray and green H_2 configurations show a 16.62% increase in fuel cost per flight when compared to gray and green H_2, respectively. Even though both SOFC green and SOFC gray H_2 hybrid cost per flight are more expensive when compared to the cost of H_2-combustion for green and gray in cases (i) and (ii), a greater overall implementation cost for the cryogenic tanks and capital is to be considered in sections 3.1.2 and 3.1.2.

Table 3.14: Fuel cost of all configurations

Fuel Type	Case	Short Haul ($)	Medium Haul ($)	Long Haul ($)
Jet-A	-	24,434.70	49,245.54	367,069.20
Gray H_2	(i)	37,522.53	75,839.06	627,966.06
	(ii)	75,045.07	151,678.13	1,255,932.12
Green H_2	(i)	52,450.85	106,011.59	877,802.02
	(ii)	104,901.71	212,023.19	1,755,604.03
Gray H_2 SOFC	(i)	44,999.95	95,690.17	798,649.00
	(ii)	89,999.90	191,380.34	1,597,298.00
Green H_2 SOFC	(i)	62,903.16	133,760.46	1,116,391.08
	(ii)	125,806.31	267,520.91	2,232,782.15

Cryogenic Tank Cost for H_2-Combustion and SOFC Hybrid Configurations

The cost of the cryogenic tanks for H_2-combustion and SOFC hybrid configurations are the same for cases (i) and (ii) since it is not required to buy new tanks for each flight. However, this cost adds significantly to the already high H_2 fuel cost that is analyzed in 3.1.2. The cryogenic tank cost for the SOFC hybrid configuration is 18.40% less expensive than the cryogenic tanks for the H_2 configuration since they require less amount of fuel, therefore smaller tanks. The complete cost of cryogenic tanks can be seen in Table 3.15.

Table 3.15: Cryogenic tank cost of H_2-combustion and SOFC hybrid configurations

System	Case	Short Haul ($)	Medium Haul ($)	Long Haul ($)
H_2	(i) & (ii)	100,809.30	203,751.78	1,265,336.08
H_2 SOFC	(i) & (ii)	82,257.97	174,917.52	973,264.01

Capital Cost for SOFC Hybrid Configuration

Although, the SOFC hybrid cryogenic tanks are cheaper than H_2-combustion case, another cost to consider is the SOFC power train which remains the same for both cases. The change in capital cost for purchasing the SOFC hybrid results in a much higher total cost for the SOFC hybrid configurations which are analyzed next in section 3.1.2.

Table 3.16: Capital cost of SOFC power train configurations

System	Case	Short Haul ($)	Medium Haul ($)	Long Haul ($)
SOFC Power Train	(i) & (ii)	3,473,335.21	7,506,534.00	29,993,346.00

Total Cost for Short, Medium, and Long Haul Configurations

To conclude, it is observed that the total cost of either retrofitted aircraft (short, medium, and long haul) compared to the conventional kerosene powered aircraft is significantly higher, with a much higher difference for gray and green SOFC due to the capital cost of purchasing the SOFC power train. The SOFC green H_2 long haul's total cost in case (ii) is estimated to be close to 33 million USD, which is 98.90% higher than the cost of the long haul kerosene powered aircraft. The best case scenario for total cost comes from gray H_2 in case (i) with an 82.34% difference from conventional kerosene, with the trade-off of not carrying any checked-in luggage. The summation of all costs (tank, capital, and fuel) for all aircraft can be seen in Table 3.17.

Table 3.17: Total cost of all configurations

Fuel Type	Case	Short Haul ($)	Medium Haul ($)	Long Haul ($)
Jet-A	-	24,434.70	49,245.54	367,069.20
Gray H_2	(i)	138,331.84	279,590.85	1,893,302.13
	(ii)	205,711.01	415,774.97	3,020,940.11
Green H_2	(i)	153,260.16	309,763.38	2,143,138.10
	(ii)	205,711.01	415,774.97	3,020,940.11
Gray H_2 SOFC	(i)	3,600,593.14	7,777,141.69	31,765,259.01
	(ii)	3,645,593.09	7,872,831.86	32,563,908.01
Green H_2 SOFC	(i)	3,618,496.35	7,815,211.97	32,083,001.09
	(ii)	3,681,399.50	7,948,972.43	33,199,392.17

3.1.3 Emissions and Lifecycle Analysis for Short, Medium, and Long Haul Configurations

Emissions

As seen in Table 3.18, the water vapor (H_2O) emissions for the short haul per flight are 28,873.95 lbs, 80,054.44 lbs, and 43,548.34 lbs for the conventional kerosene powered aircraft, H_2-combustion and SOFC hybrid powered aircraft, respectively. The contrailing of the water vapor emissions depends on the environment, combustion temperature, altitude, and mixing line "G" shown in equation 2.11. The NO_x emissions per flight are 21.68 lbs, 20.25 lbs, and 10.9 lbs for the conventional, H_2-combustion and SOFC hybrid aircraft, respectively. Thus, hydrogen combustion for short, medium, and long haul has the highest water vapor emissions as it produces about 2.6 times more water vapor than conventional kerosene fuel per unit of energy. Moreover, NO_x emissions are highest for kerosene combustion due to more fuel being burned for a single flight.

Table 3.18: NO_x and H_2O total emissions for short, medium, and long haul aircraft

Haul	Fuel Type	NO_x (lbs)	H_2O (lbs)
Short	Jet-A	314.14	28,873.95
	H_2	119.33	80,054.44
	SOFC	65.59	43,548.34
Medium	Jet-A	674.19	58,192.40
	H_2	255.94	161,802.88
	SOFC	145.65	92,603.39
Long	Jet-A	3,384.37	241,174.14
	H_2	2,369.91	1,339,767.60
	SOFC	1.316.37	772,886.12

As expected, the conventional kerosene CO_2 emissions as seen in Fig. 3.7, are the highest when compared to the hydrogen combustion CO_2 as seen in Fig. 3.8, and the SOFC as seen in Fig. 3.9. The conventional kerosene long haul CO_2 and H_2O emissions are the highest during the cruise segments, with the second highest during the climb, as seen in Fig. 3.7. Such a result is expected since the long haul is of greater weight and therefore it requires a lot more fuel. In comparison, higher emissions of CO and HC occur during the long haul idle and descent than CO_2 and H_2O emissions, due to incomplete combustion.

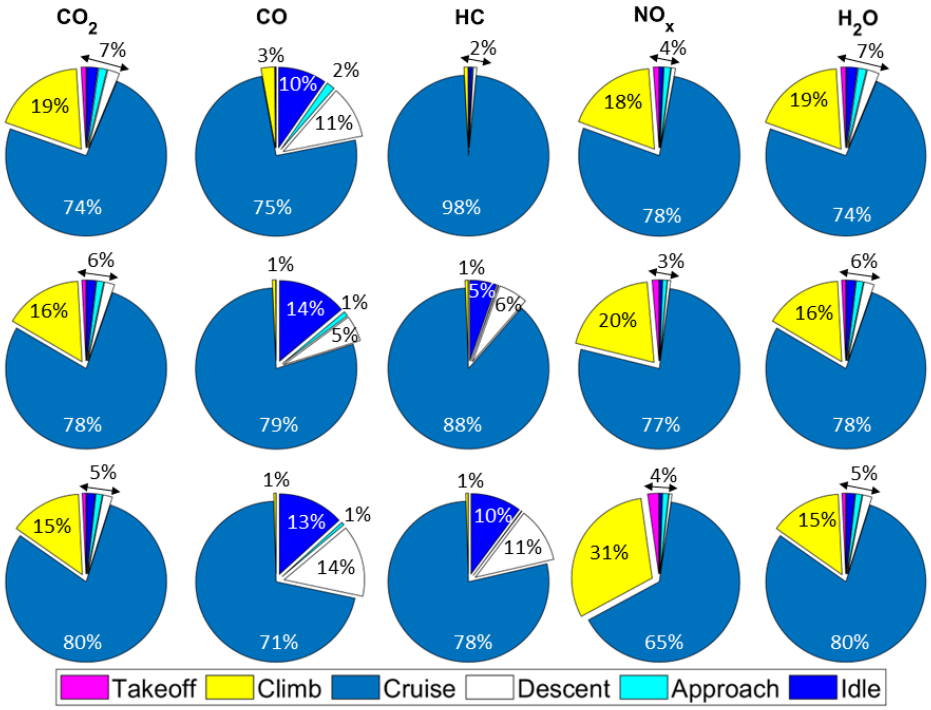

Figure 3.7: CO_2, CO, HC, NO_x, and H_2O emissions per segment of conventional kerosene for short haul (Top), medium haul (Middle), and long laul (Bottom) aircraft

Furthermore, as expected the H_2-combustion and the SOFC hybrid both result in zero CO_2 emissions during flight combustion. The long haul configuration for both H_2-combustion and SOFC hybrid have the highest water vapor emissions during the cruise segment and could therefore have a likelihood of contrail formation, as seen in Figs. 3.8 and 3.9 respectively. The second highest emissions for H_2-combustion and SOFC hybrid are the NO_x emissions,

that once again, are the highest for the long haul configuration, as it can also be observed in Table 3.18 and in Figs. 3.8 and 3.9. However, the H_2-combustion configuration for all hauls produce higher H_2O lbs emissions due to the higher amount of liquid hydrogen needed as well as having more refuel stops compared to the SOFC hybrid configuration as it is discussed in section 3.1.1.

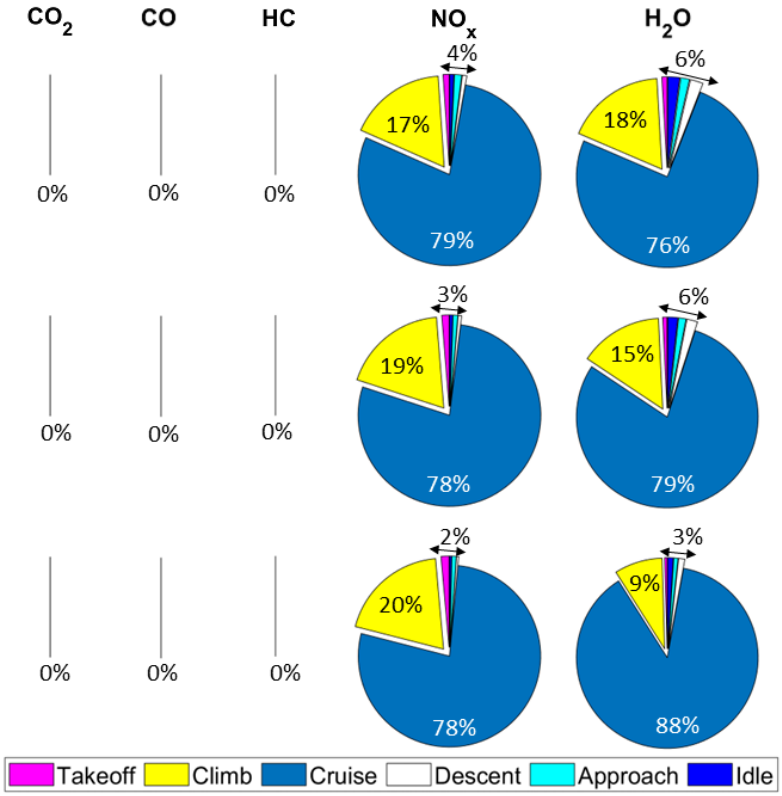

Figure 3.8: CO_2, CO, HC, NO_x, and H_2O emissions per segment of H_2-combustion for short haul (Top), medium haul (Middle), and long haul (Bottom) aircraft

When compared to a conventional aircraft, the G-factor increases due to high vapor emissions and the possibility of the low static temperature of the exhaust. In addition, fuel cells can produce condensation phenomena at the earth's surface if the weather is cold and close to frost. However, these are short-living phenomena, which will disappear after a few seconds (outside of fog), and thus the term "contrail" should not be used for such a transient phenomenon.

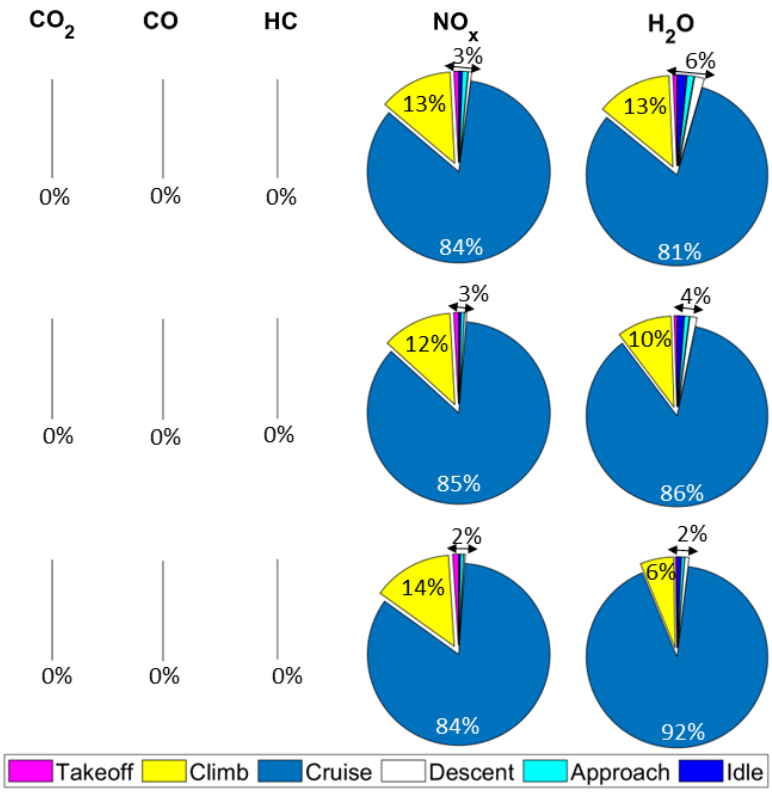

Figure 3.9: CO_2, CO, HC, NO_x, and H_2O emissions per segment of SOFC hybrid powered short haul (Top), medium haul (Middle), and long haul (Bottom) aircraft

Lifecycle

The full lifecycle of CO_2 results are categorized in two cases, as seen in Table 3.19. Case (i) for all three conventional kerosene powered configurations stands for one flight along with all the passengers and their luggage. For the retrofit H_2-combustion and SOFC hybrid short, medium, and long haul aircraft, case (i) represents one flight and their required refueling stops which can be seen in Table 3.13 along with each aircraft fixed passenger capacity without any luggage in the cargo compartment. So, case (i) accounts for one flight and the refueling stops with 76, 80, and 175 passengers for the retrofit H_2-combustion and SOFC hybrid powered short, medium, and long haul aircraft, respectively. Whereas, case (ii) models taking an additional flight for the full lifecycle of the retrofit H_2-combustion and the retrofit SOFC

hybrid aircraft in order to account the fixed number of passengers given in Table 3.1. Such a model is obtained by keeping the same original amount of passengers for the same range and adding an additional flight for both alternative fuel configurations. The results seen in Table 3.19 also show the full lifecycle as a function of the hydrogen sourcing production technique to compare emissions from both sourcing gray and green. If tank and luggage constraints did not require a second flight for the H_2 and the SOFC powered aircraft, the results would have been closer to the values obtained for all case (i) instances. In case (ii), the green retrofit SOFC hybrid powered aircraft (for all hauls) has the highest WTW by an average of 68.6% followed by the gray retrofit SOFC hybrid with an average of 51.5%, when compared to the CO_2 emissions of the kerosene powered aircraft.

Table 3.19: CO_2 emissions for full lifecycle analysis of all configurations

Fuel Type	Case	Short Haul (lbs)	Medium Haul (lbs)	Long Haul (lbs)
Jet-A	(i)	85,295.51	171,904.14	1,281,348.72
Gray H_2	(i)	80,694.88	163,097.31	1,350,485.75
	(ii)	161,389.76	326,194.62	2,700,971.50
Green H_2	(i)	44,101.11	89,135.41	738,063.09
	(ii)	88,202.21	178,270.82	1,476,126.18
Gray H_2 SOFC	(i)	43,896.73	93,344.22	779,069.22
	(ii)	87,793.45	186,688.44	1,558,138.44
Green H_2 SOFC	(i)	23,990.30	51,014.18	425,774.38
	(ii)	47,980.59	102,028.36	851,548.76

The WTW short haul percent differences in emissions lifecycles are compared with each other in Table 3.20. The maximum percent difference for case (i) is found to be 71.87% between the conventional kerosene and the green H_2 SOFC for the short haul, which is to be expected since fewer carbon emissions are omitted. The minimum percent difference for

case (ii) is obtained to be 5.40% between the conventional kerosene and the gray H_2. For case (i), the maximum percent difference is found to be 70.27% between the green H_2 SOFC and gray H_2 due to the higher emission CO_2 of gray H_2 from extraction to combustion. The minimum percent difference is found to be 0.46% between the gray H_2 SOFC and the green H_2 due to the higher CO_2 emission produced from gray H_2 extraction to combustion. The most favorable option lifecycle CO_2 emissions reduction opportunity is found for the green H_2 SOFC for case (i).

Table 3.20: % Difference between WTW short haul lifecycles

Fuel Type	Case	Jet-A (%)	Gray H_2 (%)	Green H_2 (%)	Gray H_2 SOFC (%)	Green H_2 SOFC (%)
Jet-A	(i)	-	-	-	-	-
Gray H_2	(i)	5.40	-	-	-	-
	(ii)	47.15	-	-	-	-
Green H_2	(i)	48.30	45.35	-	-	-
	(ii)	3.30	45.35	-	-	-
Gray H_2 SOFC	(i)	48.54	45.60	0.46	-	-
	(ii)	2.85	45.60	0.46	-	-
Green H_2 SOFC	(i)	71.87	70.27	45.60	45.35	-
	(ii)	43.75	70.27	45.60	45.35	-

The WTW medium haul percent differences in emissions lifecycles are compared with each other in Table 3.21. The maximum percent difference for case (i) is found to be 70.32% between the conventional kerosene and the Green H_2 SOFC for the medium haul, which is to be expected since fewer carbon emissions are omitted. The minimum percent difference for case (i) is obtained to be 5.12% between the conventional kerosene and the gray H_2. For case (ii), the maximum percent difference is found to be 68.72% between the green H_2 SOFC and gray H_2 due to the higher emission CO_2 of gray H_2 from extraction to combustion. The

minimum percent difference is found to be 4.51% between the gray H_2 SOFC and the green H_2 due to the higher CO_2 emission produced from gray H_2 extraction to combustion. The most favorable option lifecycle CO_2 emissions reduction opportunity is found for the green H_2 SOFC for case (i).

Table 3.21: % Difference between WTW medium haul lifecycles

Fuel Type	Case	Jet-A (%)	Gray H_2 (%)	Green H_2 (%)	Gray H_2 SOFC (%)	Green H_2 SOFC (%)
Jet-A	(i)	-	-	-	-	-
Gray H_2	(i)	5.12	-	-	-	-
	(ii)	47.30	-	-	-	-
Green H_2	(i)	48.15	45.35	-	-	-
	(ii)	3.57	45.35	-	-	-
Gray H_2 SOFC	(i)	45.70	42.77	4.51	-	-
	(ii)	7.92	42.77	4.51	-	-
Green H_2 SOFC	(i)	70.32	68.72	42.77	45.35	-
	(ii)	40.65	68.72	42.77	45.35	-

The WTW long haul percent differences in emissions lifecycles are compared with each other in Table 3.22. The maximum percent difference for case (i) is found to be 68.47% between the gray H_2 and the green H_2 SOFC for the long haul, which is to be expected since fewer carbon emissions are omitted. The minimum percent difference for case (i) is obtained to be 5.12% between the conventional kerosene and the gray H_2. For case (ii), the maximum percent difference is found to be 68.47% between the green H_2 SOFC and gray H_2 due to the higher emission CO_2 of gray H_2 from extraction to combustion. The minimum percent difference is found to be 5.26% between the gray H_2 SOFC and the green H_2 due to the higher CO_2 emission produced from gray H_2 extraction to combustion. The most favorable option lifecycle CO_2 emissions reduction opportunity is found for the green H_2 SOFC for

case (i).

Table 3.22: % Difference between WTW long haul lifecycles

Fuel Type	Case	Jet-A (%)	Gray H_2 (%)	Green H_2 (%)	Gray H_2 SOFC (%)	Green H_2 SOFC (%)
Jet-A	(i)	-	-	-	-	-
Gray H_2	(i)	5.12	-	-	-	-
	(ii)	52.56	-	-	-	-
Green H_2	(i)	42.40	45.35	-	-	-
	(ii)	13.20	45.35	-	-	-
Gray H_2 SOFC	(i)	39.20	42.31	5.26	-	-
	(ii)	17.76	42.31	5.26	-	-
Green H_2 SOFC	(i)	66.77	68.47	42.31	45.35	-
	(ii)	33.54	68.47	42.31	45.35	-

3.1.4 Overall Aircraft Weight Change

In case (i), the final design for both the retrofitted H_2-combustion and the SOFC hybrid resulted in the elimination of cargo space for the short, medium, and long haul configurations. The loss of the entire cargo space for the case of the H_2-combustion results in a 1.25% increase for short haul, a 27.73% decrease for medium haul, and a 38.51% decrease for the long haul in overall aircraft weight when compared to the conventional aircraft. For the SOFC hybrid configuration, such changes result in a 1.39% increase for short haul, a 0.44% decrease for medium haul, and 2.85% decrease for the long haul, in mass when compared to the conventional aircraft. For case (ii), the percent difference for the retrofitted H_2-combustion and the SOFC hybrid in comparison to the conventional aircraft have the same trend as in case (i) with slightly higher values. The complete percent differences of mass changes per

configuration and case are seen in Table 3.23, where (↑) indicates an increase in mass for the retrofitted configuration compared to the conventional powered aircraft.

Table 3.23: % Mass difference between retrofitted and conventional powered aircraft

Haul	Case	LH_2 (%)	SOFC (%)
Short	(i)	1.13(↑)	1.39(↑)
	(ii)	4.77	4.63
Medium	(i)	27.73	0.44
	(ii)	33.72	6.42
Long	(i)	38.51	2.85
	(ii)	41.45	5.79

Whereas, the highest weights for cases (i) and (ii) in the H_2-combustion for all three hauls are the empty weight and the weight of the passengers, while the main weights in the SOFC are the empty weight, passengers, and the fuel cell mass, as seen in Figs. 3.10, 3.11, and 3.12. These changes in mass are observed due to the more energy-dense hydrogen, the choice of SOA materials, for case (i) the entire loss of cargo weight and their compartments, and for case (ii) the removal of 50 percent of passengers along with their luggage plus the cargo compartment.

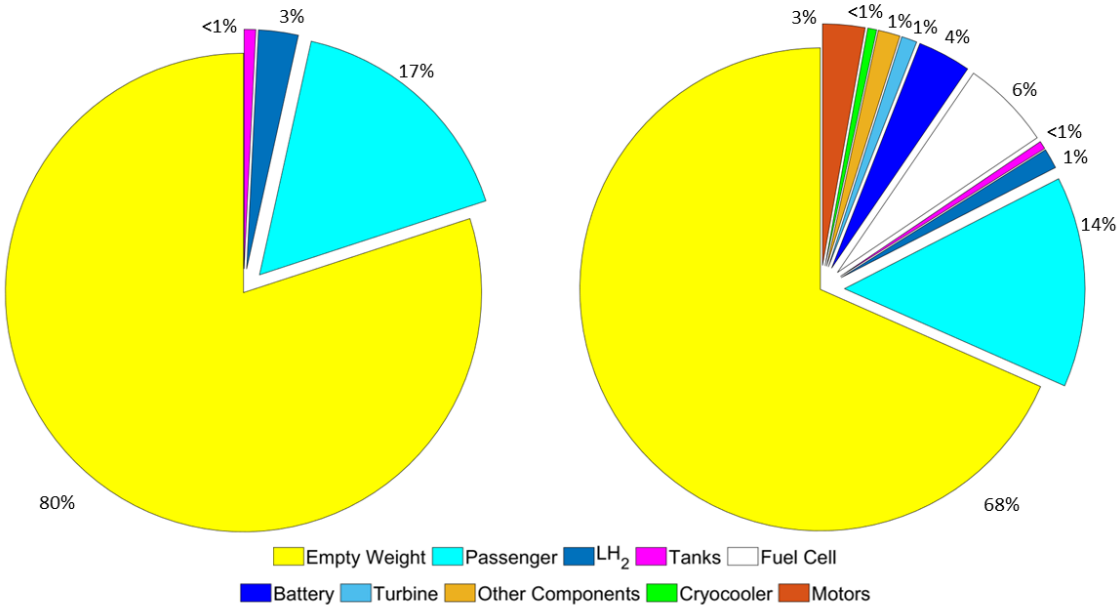

(a) Case (i)

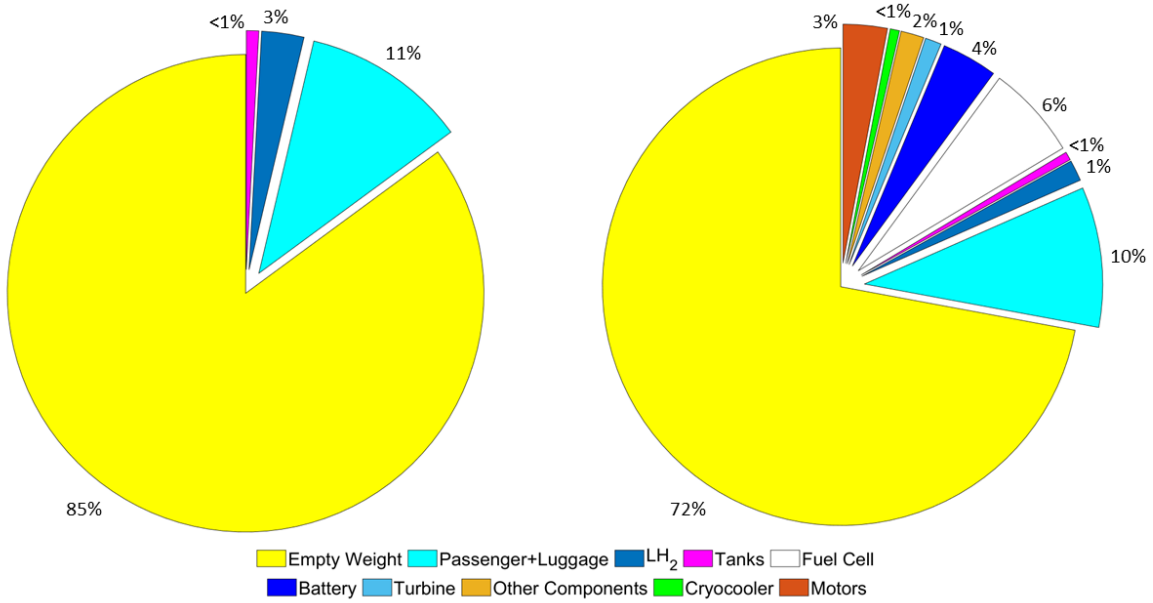

(b) Case (ii)

Figure 3.10: Resulting fractional weights from implementing a retrofit on a H_2-combustion (Left) and a SOFC hybrid (Right) powered Embraer 170LR

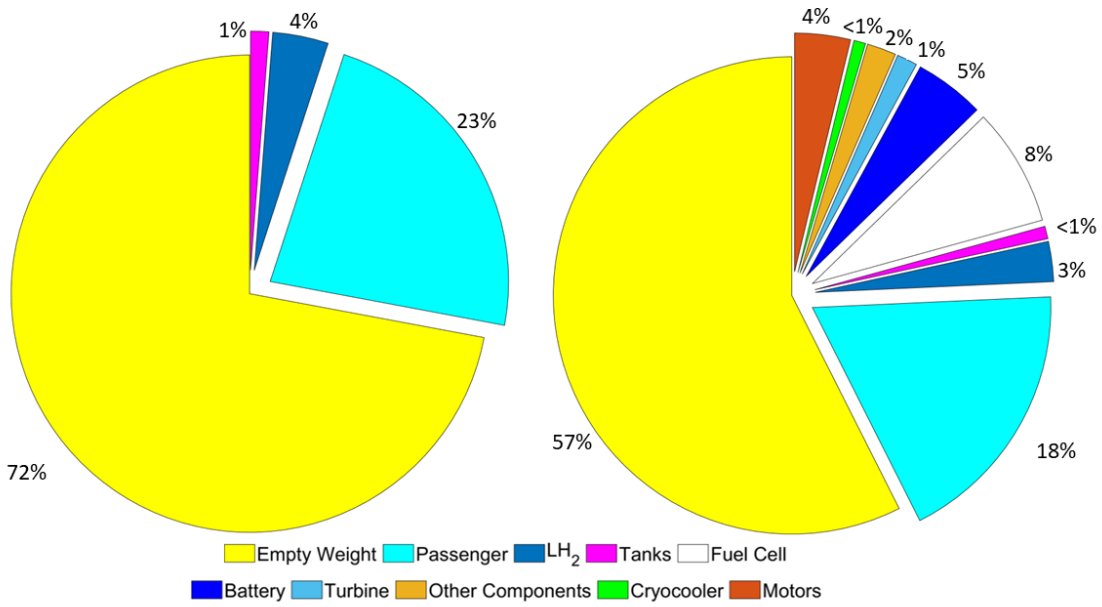

(a) Case (i)

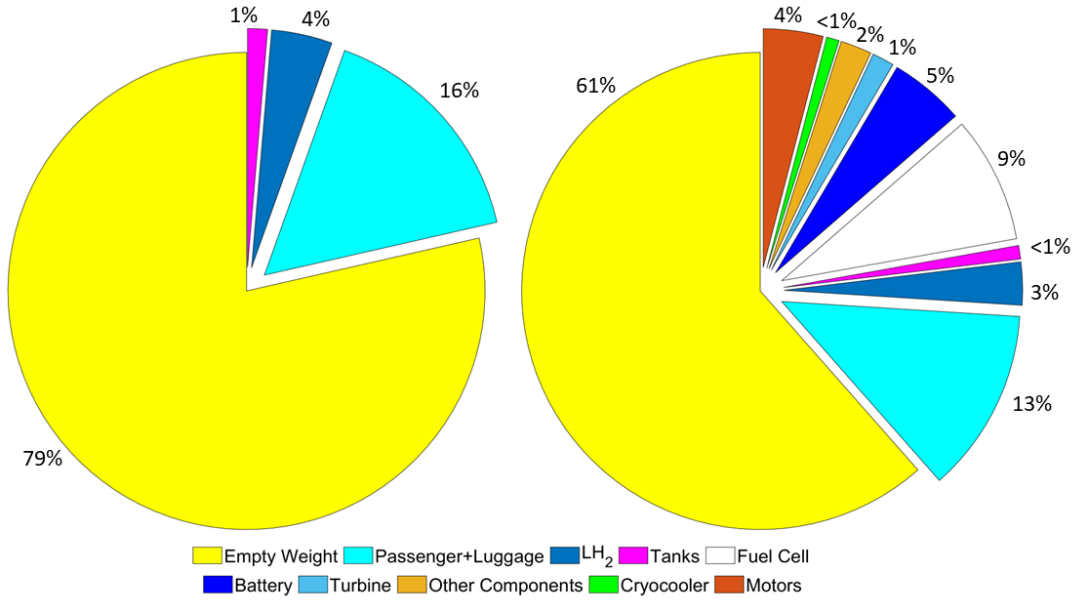

(b) Case (ii)

Figure 3.11: Resulting fractional weights from implementing a retrofit on a H_2-combustion (Left) and a SOFC hybrid (Right) powered Boeing 737-800

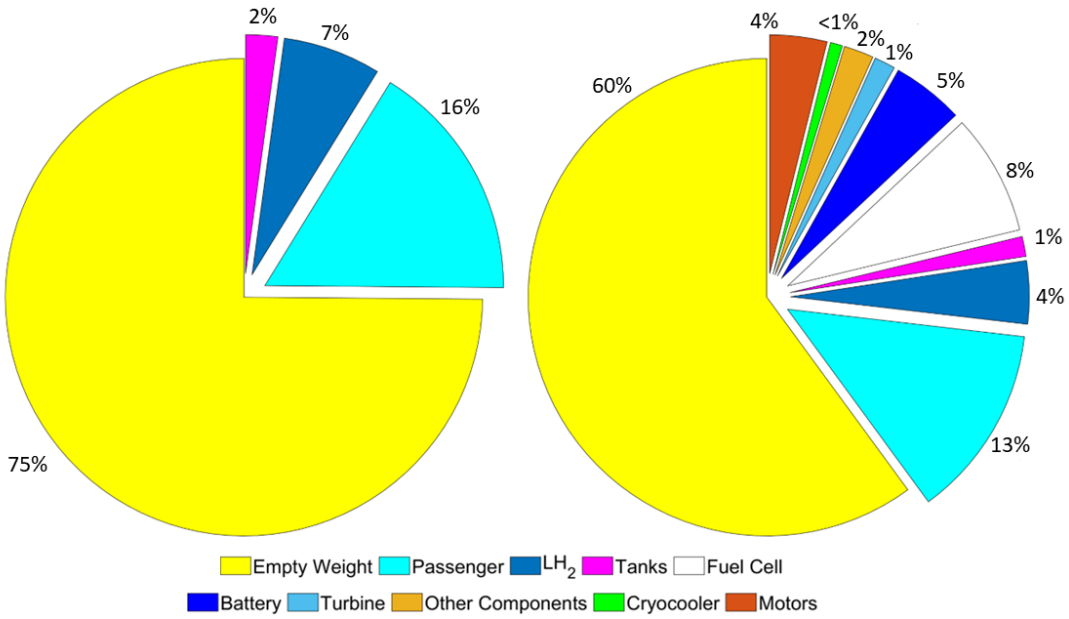

(a) Case (i)

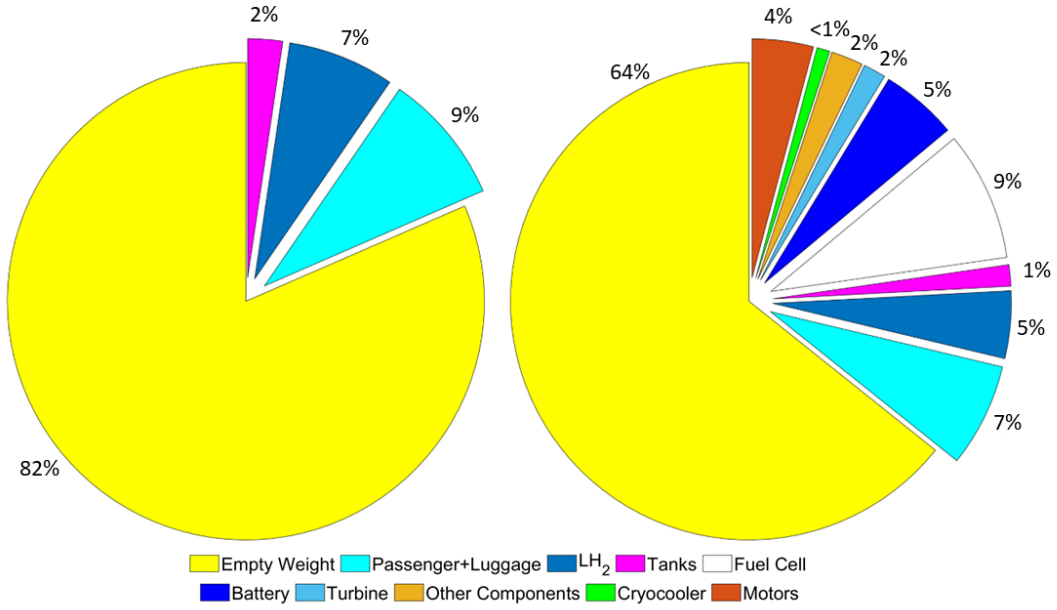

(b) Case (ii)

Figure 3.12: Resulting fractional weights from implementing a retrofit on a H_2-combustion (Left) and a SOFC hybrid (Right) powered Boeing 777-300ER

The next section 3.1.5 compares the overall results and trade-offs associated with retrofitting both commercial and business aircraft [4] in a summary. Various factors are examined, including emissions, overall weight, cost implications, lifecycle considerations, and the loss of passenger capacity. By analyzing these aspects, a comprehensive evaluation of the feasibility and benefits of retrofitting different aircraft types with alternative power systems can be obtained.

3.1.5 Comparison Between Commercial and Business Aircraft Results

In the analysis conducted in this thesis, trade-offs are identified in both case (i) and case (ii). In case (i), the trade-off involves the loss of cargo compartment space while maintaining the same number of passengers as the conventional kerosene aircraft. Additionally, passengers are required to forego their luggage in this scenario. Conversely, in case (ii), a different trade-off arises where 50% of the passengers are omitted to utilize the available cabin area for accommodating their luggage. However, to ensure a comprehensive comparison, a second flight becomes necessary to transport the remaining 50% of passengers and their luggage. It is important to note that case (ii) results in higher emissions and costs compared to case (i). A similar trade-off is observed in Alsamri's [4] analysis of business jets, where the loss of three passengers is necessary to accommodate the appropriate number of cryogenic tanks for flying the fixed range, and a second flight is considered to transport the remaining passengers. Both in this thesis and the referenced paper, the trade-off involves passenger loss in exchange for lower carbon emissions and reduced fuel costs, or in case of the case (ii), higher costs and emissions due to the second flight.

The findings and implications are in the following chapter 4 after examining the outcomes of the conducted analysis. A comprehensive examination of numerous issues such as emis-

sions, overall weight, costs, lifecycle, and their effect on passenger capacity provided useful insights. These results are combined and presented in the conclusion, which seeks to provide a thorough assessment of the trade-offs, benefits, and constraints of retrofitting commercial aircraft with alternative power sources. The conclusion's aim is to provide light on the possibility and effectiveness of these retrofitting solutions in creating more environmentally friendly and sustainable air travel.

Chapter 4

Conclusion

The proposed methodology in this thesis models the performance, lifecycle emissions, and costs of retrofitting three aircraft with H_2-combustion and SOFC hybrid power systems. The methodology includes a constant range and airframe analysis to design liquid hydrogen fuel tanks that meet insulation, sizing, center of gravity, and power constraints. However, achieving the desired mass change involves making refueling stops and sacrificing baggage space to accommodate cryogenic tank sizing and weight constraints for the same range. As a result, both H_2-combustion and SOFC hybrid aircraft cannot carry the same amount of baggage as kerosene-powered aircraft for the same range. In case (ii) analysis, a second flight is required to accommodate the remaining passengers. This doubling of emissions and fuel costs in case (ii) diminishes the viability of the retrofit solution, even though all passengers can fly similarly to conventional aircraft. The limitations on cargo space due to cryogenic tanks result in the need for additional flights, which impacts emissions and costs.

While kerosene-powered aircraft can transport more baggage per trip, they have higher carbon emissions. Compared to retrofit aircraft in case (i), conventional kerosene combustion results in the highest WTW CO_2 lbs emissions of 85,295.51 lbs, 171,904.14 lbs, and

1,281,348.72 lbs per flight for the short, medium, and long haul configurations, respectively. Therefore, utilizing hydrogen alternative fuels provides a significant advantage for potential carbon mitigation since kerosene combustion also produces other greenhouse gas (GHG) emissions besides NO_x, CO_2, and H_2O that are shared by all systems. The NO_x emissions are highest in conventional aircraft and lower in hydrogen combustion and SOFC hybrid aircraft, respectively. Gray and green hydrogen combustion in case (i) yield 5.40% and 48.30% lower WTW CO_2 lbs emissions compared to kerosene for the short haul case. However, that is not true for case (ii), where they yield 47.15% and 3.30% higher WTW CO_2 lbs emissions. Similarly, in case (i) for the medium haul configuration, gray and green hydrogen-powered SOFC hybrids exhibit a 45.70% and 70.32% reduction in WTW CO_2 lbs emissions compared to conventional kerosene, respectively. In case (ii), gray and green hydrogen-powered SOFC hybrids exhibit a 7.92% increase and a 40.65% reduction in WTW CO_2 lbs emissions compared to conventional kerosene.Therefore, the SOFC hybrid aircraft powered by green hydrogen is the best option in terms of CO_2 emissions for cases (i) and (ii).

However, it is necessary to evaluate other greenhouse emissions when comparing the SOFC hybrid to H_2-combustion. H_2O TTW emissions are highest for H_2-combustion aircraft, which increases the likelihood of contrail formation. While water vapor does not have a permanent climate effect like CO_2 emissions, the radiative forcing caused by contrails has a similar magnitude to CO_2 emissions from kerosene combustion. Therefore, potential solutions to address this concern include avoiding night-time flights and flying at lower altitudes.

Another consideration is the change in fuel cost required to accommodate the fixed ranges when replacing kerosene-powered aircraft. All alternative power systems, including gray and green H_2 and SOFC H_2 hybrids, show a significant cost increase compared to kerosene fuel. This increase is due to the higher cost of green H_2 production and, primarily, the need for refueling stops. The SOFC H_2 gray hybrid for the short haul aircraft offers the cheapest change in fuel price per flight. However, there is a higher one-time capital cost of

3,473,335.21 USD associated with purchasing the SOFC power train. Although the SOFC hybrid powered aircraft presents a greater potential for lowering carbon emissions, it also incurs a higher change in fuel cost to cover the entire fixed range compared to kerosene. This trade-off allows for carbon mitigation in the near future but requires sacrificing a percentage of baggage capacity for the same range.

Taking into account the proposed methodology and its analysis of retrofitting aircraft with H_2-combustion and SOFC hybrid power systems, it becomes evident that a comprehensive approach is necessary to achieve a greener aviation industry. While retrofitting alone, as demonstrated in case (i), may result in lower carbon emissions, it is crucial to consider other variables such as aircraft size and engine types (turbofan, turbojet, and turboprop) for the widespread implementation of alternative propulsive and aircraft power systems. The methodology presented in this thesis serves as a framework that can be applied to any aircraft category and engine type, allowing for a systematic evaluation of retrofitting possibilities. These findings highlight the environmental advantages of LH_2 fuel arrangements but also emphasize the trade-off of decreased cargo compartment capacity. As humanity strives for a greener future, further research is needed to optimize LH_2 storage systems, minimizing the impact on cargo compartment capacity while maintaining a balance between emission reduction and passenger convenience. Continued efforts in researching and pursuing low-emission aviation technologies will contribute to a more sustainable aviation industry, addressing the imperative goal of reducing CO_2 emissions and creating a more environmentally conscious future for air travel.

Bibliography

[1] Roger D. Schaufele. *Elements of Aircraft Preliminary Design*. Aries Publications, 2000.

[2] Oliver Wyman. Aviation sustainability: Our future, 2022.

[3] Andrew Gong and Dries Verstraete. Fuel cell propulsion in small fixed-wing unmanned aerial vehicles: Current status and research needs. *International Journal of Hydrogen Energy*, 42(33):21311–21333, 2017.

[4] K. Alsamri and *et al.* Methodology for assessing retrofitted hydrogen combustion and fuel cell aircraft environmental impacts. AIAA 2022-3508, AIAA Aviation, 2022.

[5] VistaJet. Aviation's impact on tomorrow. *VistaJet: Sustainability in Aviation*, 2022.

[6] H. Nojoumi, I. Dincer, and G.F. Naterer. Greenhouse gas emissions assessment of hydrogen and kerosene-fueled aircraft propulsion. *International Journal of Hydrogen Energy*, 34(3):1363–1369, 2009.

[7] Yize Liu, Xiaoxiao Sun, Vishal Sethi, Devaiah Nalianda, Yiguang Li, and Lu Wang. Review of modern low emissions combustion technologies for aero gas turbine engines. *Progress in Aerospace Sciences*, 94, 09 2017.

[8] Rajesh Ahluwalia, Thanh Hua, J.-K Peng, Sanaa Lasher, K. McKenney, J. Sinha, and Monterey Gardiner. Technical assessment of cryo-compressed hydrogen storage tank systems for automotive applications. *International Journal of Hydrogen Energy*, 35:4171–4184, 01 2011.

[9] ian douglas. Aircraft emissions - nav node dlr portal, 2002.

[10] Robert Tornabene, Xiao-yen Wang, Steffen, Christopher J, and Joshua Freeh. Development of parametric mass and volume models for an aerospace sofc/gas turbine hybrid system. 08 2005.

[11] NASA. High power density solid oxide fuel cell. Online, 2016. https://technology.nasa.gov/patent/LEW-TOPS-120.

[12] Ahmad Baroutaji, Tabbi Wilberforce Awotwe, Mohamad Ramadan, and Abdul Ghani Olabi. Comprehensive investigation on hydrogen and fuel cell technology in the aviation and aerospace sectors. *Renewable and Sustainable Energy Reviews*, 106:31–40, 05 2019.

[13] Christopher Winnefeld, Thomas Kadyk, Boris Bensmann, Ulrike Krewer, and Richard Hanke-Rauschenbach. Modelling and designing cryogenic hydrogen tanks for future aircraft applications. *Energies*, 11:105, 01 2018.

[14] D. Verstraete, Cranfield University. School of Engineering, and K. Ramsden. *Potential of Liquid Hydrogen for Long Range Aircraft Propulsion*. Theses 2009. Cranfield University, School of Engineering, Gas Turbine Engineering, 2009.

[15] Anthony J. Colozza and Lisa Kohout. Hydrogen storage for aircraft applications overview. Contractor report (cr), Analex Corp. Brook Park, OH United States, November 2002. NASA/CR-2002-211867.

[16] U.S. Department of Transportation. Federal Aviation Administration Aircraft Weight and Balance Handbook. Online, 2016.

[17] Richard S. Shevell. *Fundamental Principles of Flight*. Prentice Hall, 1989.

[18] Embraer Commercial Aviation. E170, n.d.

[19] Flugzeuginfo. Boeing 737-800, n.d.

[20] Boeing. Boeing 777, n.d.

[21] Ilissa B Ocko and Steven P Hamburg. Climate consequences of hydrogen emissions. *Atmospheric Chemistry and Physics*, 22(14):9349–9368, 2022.

[22] M. Anwar H. Khan, Joel Brierley, Kieran N. Tait, Steve Bullock, Dudley E. Shallcross, and Mark H. Lowenberg. The emissions of water vapour and nox from modelled hydrogen-fuelled aircraft and the impact of nox reduction on climate compared with kerosene-fuelled aircraft. *Atmosphere*, 13(10), 2022.

[23] Kolja Seeckt and Dieter Scholz. Jet versus prop, hydrogen versus kerosene for a regional freighter aircraft. 2009.

[24] Klaus Gierens. Theory of contrail formation for fuel cells. *Aerospace*, 8(6), 2021.

[25] M. E. J. Stettler, G. S. Koudis, S. J. Hu, A. Majumdar, and W. Y. Ochieng. The impact of single engine taxiing on aircraft fuel consumption and pollutant emissions. *The Aeronautical Journal*, 122(1258):1967–1984, 2018.

[26] Yashovardhan Chati and Hamsa Balakrishnan. Analysis of aircraft fuel burn and emissions in the landing and take off cycle using operational data. 05 2014.

[27] Gillian Whelan, Fiona Cawkwell, Hermann Mannstein, and Patrick Minnis. The use of meteorological data to improve contrail detection in thermal imagery over ireland. 09 2009.

[28] Douglas Spangenberg, Patrick Minnis, Sarah Bedka, Rabindra Palikonda, David Duda, and Fred Rose. Contrail radiative forcing over the northern hemisphere from 2006 aqua modis data. *Geophysical Research Letters*, 40:595–600, 02 2013.

[29] C. Koroneos, A. Dompros, G. Roumbas, and N. Moussiopoulos. Advantages of the use of hydrogen fuel as compared to kerosene. *Resources, Conservation and Recycling*, 44(2):99–113, 2005.

[30] Stephanie Searle Nikita Pavlenko. Assessing the sustainability implications of alternative aviation fuels. *2021 INTERNATIONAL COUNCIL ON CLEAN TRANSPORTATION*, March 2021.

[31] Michael Wang, Amgad Elgowainy, Z Lu, Adarsh Bafana, PT Benavides, Andrew Burnham, Hao Cai, Qiang Dai, Ulises Gracida, TR Hawkins, et al. Greenhouse gases, regulated emissions, and energy use in technologies model®(2020. net). *Computer software]. https://doi. org/10.11578/GREET-Net-2020/dc*, 20200913, 2020.

[32] G. Kakoulaki, I. Kougias, N. Taylor, F. Dolci, J. Moya, and A. Jäger-Waldau. Green hydrogen in europe – a regional assessment: Substituting existing production with electrolysis powered by renewables. *Energy Conversion and Management*, 228:113649, 2021.

[33] Mohammed Al-Breiki and Yusuf Bicer. Comparative life cycle assessment of sustainable energy carriers including production, storage, overseas transport and utilization. *Journal of Cleaner Production*, 279:123481, 2021.

[34] Robert W. Howarth and Mark Z. Jacobson. How green is blue hydrogen. *Energy Science & Engineering*, 9(10):1676–1687.

[35] Types of hydrogen production. Johnson Matthey Journal, 2019.

[36] Elizabeth Connelly, Michael Penev, Amgad Elgowainy, and Chad Hunter. Current status of hydrogen liquefaction costs. *DOE Hydrogen and Fuel Cells Program Record*, pages 1–10, 2019.

[37] J. Hoelzen, D. Silberhorn, T. Zill, B. Bensmann, and R. Hanke-Rauschenbach. Hydrogen-powered aviation and its reliance on green hydrogen infrastructure – review and research gaps. *International Journal of Hydrogen Energy*, 47(5):3108–3130, 2022. Hydrogen Energy and Fuel Cells.

[38] Boning Yang, Muharrem Mane, and William Crossley. An approach to evaluate fleet level co2 impact of introducing liquid-hydrogen aircraft to a world-wide network. 06 2022.

[39] Roberto Scataglini and et al. A total cost of ownership model for solid oxide fuel cells in combined heat and power and power only applications, 2015.

[40] Barney L. Capehart. Microturbines, Dec 2016.

[41] Statista. Lithium ion battery pack costs, Jul 2022.